# Downregulation of MMP1 expression mediates the anti-aging activity of Citrus sinensis peel extract nanoformulation in UV induced photoaging in mice

**Article** *in* Biomedicine & Pharmacotherapy · March 2021

DOI: 10.1016/j.biopha.2021.111537

CITATIONS
0

**9 authors**, including:

Dalia AbdelRhman Attia
The British University in Egypt BUE
**27** PUBLICATIONS **239** CITATIONS

SEE PROFILE

Biomedicine & Pharmacotherapy 138 (2021) 111537

Contents lists available at ScienceDirect

Biomedicine & Pharmacotherapy

journal homepage: www.elsevier.com/locate/biopha

Original article

# Downregulation of MMP1 expression mediates the anti-aging activity of *Citrus sinensis* peel extract nanoformulation in UV induced photoaging in mice

Reham I. Amer [a,b], Shahira M. Ezzat [c,d,*], Nora M. Aborehab [e], Mai F. Ragab [f], Dalia Mohamed [g,h], Amira Hashad [b], Dalia Attia [i], Maha M. Salama [c,j], Mahitab H. El Bishbishy [d]

[a] Department of Pharmaceutics and Industrial Pharmacy, Faculty of Pharmacy, Al-Azhar University, Cairo, Egypt
[b] Department of Pharmaceutics, Faculty of Pharmacy, October University for Modern Sciences and Arts (MSA), Giza 12451, Egypt
[c] Department of Pharmacognosy, Faculty of Pharmacy, Cairo University, Kasr El-Aini Street, Cairo 11562, Egypt
[d] Department of Pharmacognosy, Faculty of Pharmacy, October University for Modern Sciences and Arts (MSA), Giza 12451, Egypt
[e] Department of Biochemistry, Faculty of Pharmacy, October University for Modern Sciences and Arts (MSA), Giza 12451, Egypt
[f] Department of Pharmacology and Toxicology, Faculty of Pharmacy, October University for Modern Sciences and Arts (MSA), Giza 12451, Egypt
[g] Department of Analytical Chemistry, Faculty of Pharmacy, Helwan University, Ein Helwan, Cairo 11795, Egypt
[h] Department of Analytical Chemistry, Faculty of Pharmacy, October University for Modern Sciences and Arts (MSA), Giza 12451, Egypt
[i] Department of Pharmaceutics, Faculty of Pharmacy, The British University in Egypt, El Sherouk City, Suez Desert Road, Cairo 11837, Egypt
[j] Department of Pharmacognosy, Faculty of Pharmacy, The British University in Egypt, El Sherouk City, Suez Desert Road, Cairo 11837, Egypt

ARTICLE INFO

*Keywords:*
Skin aging
Lipid nanoparticles
Factorial Design
*Citrus sinensis* L.
Elastase
Collagenase

ABSTRACT

Aging of the skin is a complicated bioprocess that is affected by constant exposure to ultraviolet irradiation. The application of herbal-based anti-aging creams is still the best choice for treatment. In the present study, *Citrus sinensis* L. fruit peels ethanolic extract (CSPE) was formulated into lipid nanoparticles (LNPs) anti-aging cream. Eight different formulations of CSEP-LNPs were prepared and optimized using $2^3$ full factorial designs. *In vivo* antiaging effect of the best formula was tested in Swiss albino mice where photo-aging was induced by exposure to UV radiation. HPLC-QToF-MS/MS metabolic profiling of CSPE led to the identification of twenty-nine metabolites. CSPE was standardized to a hesperidin content of 15.53 ± 0.152 mg% using RP-HPLC. It was suggested that the optimized formulation (F7) had (245 nm) particle size, (91.065%) EE, and (91.385%) occlusive effect with a spherical and smooth surface. The visible appearance of UV-induced photoaging in mice was significantly improved after topical application on CSPE-NLC cream for 5 weeks, levels of collagen and SOD were significantly increased in CSPE- NLC group, while levels of PGE2, COX2, JNK, MDA, and elastin was reduced. Finally, The prepared anti-aging CSPE-NLC cream represents a safe, convenient, and promising skincare cosmetic product.

## 1. Introduction

Skin aging is a result of a lot of factors including ultraviolet radiation (UV), excessive alcohol intake, smoking, and environmental pollutants. A combination of these factors leads to cumulative deterioration in cellular DNA and skin protein [1]. Skin aging is characterized by dryness, irregular pigmentation as well as fine wrinkling caused by disorganization of epidermis and dermis composition accompanying by loss of elasticity, and roughness [2].

Recently, a hobby for youth and beauty has become a vital issue of women. Enhancement of the visible signs of aging has taken a remarkable concern that affected the quality of women's life. Utilizing cosmetic products with different mechanisms improve skin beauty and desirability, so it protects skin aging. Nowadays, consumers have motivated the use of natural ingredients such as herbal extract in skin care products especially the topical application of antioxidants, anti-inflammatory, moisturizing and UV-protective, proved their popularity as a fruitful anti-aging medication Saraf and Kaur [3].

According to [4], several plants were used in the treatment of wrinkles Aloe (*Aloe vera*), Wheat (*Triticum sativum*), Japanese red pine (*Pinus densiflors*), Cucumber (*Curcumis sativum*), Rosemary (*Rosmarinus officinalis*), Wild Carrot (*Daucus carota*), Coriander (*Coriandrum sativum*)

* Correspondence to: Department of Pharmacognosy, Faculty of Pharmacy, Cairo University, Cairo 11562, Egypt.
*E-mail address:* shahira.ezzat@pharma.cu.edu.eg (S.M. Ezzat).

https://doi.org/10.1016/j.biopha.2021.111537
Received 20 January 2021; Received in revised form 13 March 2021; Accepted 21 March 2021

and Sweet orange (*Citrus sinensis*). Owing to their metabolites, these plants possess promising anti-wrinkles activity through different mechanisms such as; increasing formation of collagen fibers in the dermis, decreasing the expression of collagenase and/or matrix metalloproteinase as well as their radical scavenging activities. *C. sinensis* L. peels were selected for this study as it is well-known to exhibit potent antioxidant effect due to its rich content of vitamin C [5], also orange peels are considered waste products produced in huge amounts and thus should be regarded as a value-added product.

Citrus represents an important economic Egyptian fruit crop. Egypt ranks the 6th largest orange exporter and producer worldwide[6]. In 2019/2020, Foreign Agriculture Service (FAS) Cairo forecasts fresh orange exports to reach 1.5MMT. Among different Citrus species growing in Egypt, orange represents the main species that occupy 69% of the cultivated citrus Fields. *Citrus sinesis* L. Family Rutaceae (Navel orange) is the major species of citrus cultivated in Egypt especially in the Delta (occupies 60% of the cultivated area) and also ranked number one in production (60%) [7].

Nanotechnology is a beneficial science that involves the design and application of innovative controlled nonmetric size particles for the treatment of both health and beauty complication. Therefore, it has a wide range of uses in many different fields; especially the pharmaceutical field and cosmetics due to its remarkable advantageous properties [8].

Lipid nanoparticles (LNPs) are the most common type of colloidal nanoparticle systems intentional for topical application. Nanostructured lipid carriers (NLC) and solid lipid nanoparticles (SLN) are the most suitable carriers for skin applications [9]. As they are relatively simple to prepare on large scale and also cheap [10] and increasing in drug penetration due to occlusive properties and moisturizing effect of SLN and NLC on the skin. Additionally; they can deliver medications into the deeper layers of the skin and offer a reservoir effect so sustained drug release. They are based on non-irritant and non-toxic lipids. Thus, SLN and NLC formulations have been recommended to be suitable for cosmeceuticals that are intended to persist in the skin without permeation, thereby minimizing their systemic effects.

Giving these properties the objective of the present study was to develop and optimize different formulations of *Citrus sinensis* L. peels standardized ethanolic extract (CSPE) loaded SLN and NLC using $2^3$ factorial design to enhance its topical anti-aging effect. Further, based on particle size, encapsulation efficiency, and skin occlusive effect, the optimized CSPE -lipid nanoparticles (CSPE-LNP) dispersion was selected and formulated into a topical cream. Drug content and in-vitro permeation study were done on the prepared anti-aging CSPE-LNP cream. The CSPE's chemical profile was also achieved via HPLC-QToF MS-MS to identify major metabolites.

UV photo-aging was induced in the mice model to evaluate the possible mechanism by which CSPE-NLC produces its beneficial anti-aging activity.

## 2. Material and methods

### 2.1. Plant material and extraction procedure

The *Citrus sinensis* L. fruits were obtained from Agricultural Research Center, Giza, Egypt allocated in "9, Cairo University Road, Oula, Giza District, Giza Governorate". The taxonomical identity was kindly verified by Dr. Reem Samir Hamdy, Lecturer of Plant Taxonomy, Botany Department, Faculty of Science, Cairo University. A voucher specimen (2–2–2014) was deposited at the Museum of the Pharmacognosy Department, Faculty of Pharmacy, Cairo University.

The peels were separated from the flesh and dried in shade to obtain 3 kg dried peels. The peels were grinded and extracted by 95% ethanol. The ethanolic extracts were combined and concentrated under reduced pressure at 45 °C using a rotary evaporator to obtain 500 g dry ethanolic residue of *Citrus sinensis* peels (CSPE). CSPE was placed in a refrigerator in a tightly closed amber glass container.

### 2.2. Chemicals and reagents

Cocoa butter (Aboca S.p.A., Sansepolcro, Italy), olive oil was kindly supplied by Eipico (Cairo, Egypt), L-α-phosphatidylcholine (L-α-lecithin) and tween80 were purchased from Sigma-Aldrich Chemical Co. (St Louis, MO, USA). Ethanol, methanol, stearic acid, sodium bicarbonate, glycerin, and potassium hydroxide were provided by El-Nasr Chemical Co (Cairo, Egypt). A Spectrapore® nitrocellulose membrane (15,000 Mw cutoffs) was purchased from Spectrapore Inc. (New York, NY, USA). Chemicals for the Elastase inhibition assays (human leukocyte elastase, 4-(2-hydroxyethyl)- 1-piperazineethane sulfonic acid (HEPES) buffer (pH 7.5), N-Methoxysuccinyl-Ala-Ala-Pro-Val-p-nitroanilide (the substrate) and collagenase inhibition assays (collagenase type 1 from Clostridium histolyticum, tris (hydroxymethyl)-methyl-2-aminoethane sulfonate (TES) buffer (50 mM) with 0.36 mM calcium chloride (pH 7.4), EGCG, and the substrate N-[3-(2-furyl)acryloyl]-Leu-Gly-Pro-Ala (FALGPA), citrate buffer (pH 5) and ninhydrin) as well as materials for ORAC assay viz. 2,2-azobis (2-amidinopropane) dihydrochloride, fluorescein, phosphate buffer (PH7.4) and Trolox were purchased from Sigma-Aldrich Chemical Co. (St Louis, MO, USA). DPPH (2, 2-diphenyl-1-picryl hydrazyl) and ascorbic acid were purchased from Sigma-Aldrich Chemical Co. (St Louis, MO, USA). All solvents used were of HPLC grade; methanol, acetonitrile, and formic acid were purchased from Sigma-Aldrich Chemical Co. (St Louis, MO, USA).

### 2.3. HPLC- Quadrupole Time-of-Flight -Mass Spectroscopy (HPLC-QToFMS-MS) apparatus

The ethanolic extract was prepared at a concentration of 1 μg/μl in distilled water: methanol: acetonitrile (50: 25: 25 v:v:v) solution, centrifuged, and degassing was done by sonication. HPLC-QTOF/MS-MS analysis was carried out on a Waters® XBridge C18 column, (3.5 μm - 2.1 × 50 mm, i.d.), with an integrated pre-column Phenomenex® In-Line filter disks. The injection volume (10 μl) was eluted using two eluents: eluent A is nano-pure $H_2O$ acidified with 0.1% formic acid and eluent B is 100% acetonitrile with the flow rate of 0.3 mL/min in 28 min. A Sciex® TripleTOF 5600 + mass spectrometer was used for MS analysis in a positive ion mode and full scan mode in the mass range *m/z* 50–1000. The peaks and spectra were processed using the MarkerView1.3, Sciex® software, and assigned by comparison of their retention times ($R_t$) and MS with published data.

### 2.4. In vitro antioxidant activity

Radical scavenging activity of CSP was measured against DPPH spectrophotometrically, ascorbic acid was used as a positive control [11]. CS was dissolved in a concentration of 1000 μg/mL in ethanol. From this solution, the other tested dilutions of the extract were prepared (0.5 −500 μg/mL). The final concentration of DPPH in the reaction mixture was 0.125 mM. After incubation of the mixture at 37 °C for 30 min in the dark, the absorbance was measured at 517 nm. Blank samples contained the same amount of ethanol and DPPH solution. All experiments were carried out in triplicate. Ascorbic acid was used as a positive control. Percentage radical scavenging activity of samples was calculated using the following formula:

$$\text{Radical Scavenging Activity}(\%) = \left[\frac{(A_{Blank} - A_{Sample})}{A_{Blank}}\right]100$$

$ED_{50}$ values, the concentration of the sample that causes 50% loss of the DPPH activity (colour).

Besides, the Oxygen Radical Absorbance Capacity (ORAC) was determined for CSPE, where the extract was dissolved in phosphate-buffered saline (10 mM, pH 7.4) and investigated for its antioxidant

capacity [12] using Trolox as a positive control. The antioxidant activity is represented as the percentage inhibition of fluorescence decay. The experiment was performed using 96 well plates (Corning Costar Corporation, Cambridge, MA, cat. no. 3792). In each well, 150 μl of 2.5 nM fluorescein, 25 μl Trolox (final concentrations: 0.78–25 μM) or 25 μl tested extract were pipetted in quadruplicate. The plate was allowed to equilibrate at 37 °C for 30 min. Every 90-sec fluorescence measurements (Ex. 485 nm, Em. 520 nm) were done. After three cycles we used the multi-channel-pipette to add 25 μl AAPH (60 mM) were to each well. After taking these measurements for 90 min, $ED_{50}$ values were calculated.

### 2.5. In-vitro evaluation of anti-elastase activity

Working solutions were prepared using samples of CSPE at concentrations of 50–500 μg/mL dissolved in water. The assay was performed according to the published method using Elafin as a positive control [13].

### 2.6. In-vitro evaluation of anti-collagenase activity

Working solutions were prepared using samples of CSPE at concentrations of 50 – 500 μg/mL dissolved in water. the collagenase inhibition assay of [13] was applied using epigallocatechin gallate (EGCG) as the positive control.

### 2.7. HPLC standardization of the CSPE

#### 2.7.1. Sample preparation

CSPE stock solution (10 mg/mL): 0.25 g extract was dissolved in 20 mL methanol under sonication for 15 min. The extract was then filtered in a 25 mL volumetric flask followed by completing the volume using methanol.

Hesperidin standard stock solution (1 mg/mL): 50 mg hesperidin was dissolved in 30 mL methanol under sonication for 15 min. Then the solution was filtered in a 50-mL volumetric flask followed by completing the volume using methanol.

#### 2.7.2. Chromatographic conditions

The utilized HPLC system was; Agilent 1200 series (Model G1329A). Agilent 1200 series autosampler was used for sample injection, while Agilent ChemStation software, version A.10.01 was used for data collection and processing. The stationary phase was Gemimi C18 Column (150 × 4.6 mm, 5 μm), Phenomenex, USA. The temperature was adjusted at $35^0$ C. The mobile phase composed of aqueous 0.1% formic acid (A): acetonitrile (B): methanol (C) was run using the following gradient elution program; from 0 to 5 min (90 A: 10 B: 0 C) then, from 5 to 20 min (85 A: 15 B: 0 C), then, from 20 to 60 min (55 A: 25 B: 20 C). The mobile phase was filtered with a 0.45 μm Millipore membrane filter (Billerica, MA) before its injection. The flow rate was 1.5 mL/min, the injection volume was 20 μl and the detection was performed at 280 nm. Hesperidin was eluted at 24.034 min

#### 2.7.3. Construction of hesperidin calibration curve

Aliquots equivalent to 0.1–2.0 mL were relocated from hesperidin stock solution (1 mg/mL) in a series of 10-mL volumetric flasks. The chromatograms for the prepared hesperidin solutions were recorded by applying the previously described chromatographic conditions. The construction of hesperidin calibration curve was performed by plotting the peak area of each solution against the equivalent concentration, from which the regression equation was computed. The calibration curve showed a linear relationship in the range of 10–200 μg/mL.

#### 2.7.4. Validation of the chromatographic method

The accuracy, intraday, and inter-day precision of the chromatographic method were evaluated through triplicate analysis of three hesperidin concentrations (40, 80, 160 μg/mL) on same/different days followed by the calculation of the Recovery %, the standard deviation (SD) and the percentage relative standard deviation (%RSD). The robustness of the method was assessed by analyzing the same three concentrations in triplicate but after applying intended minor changes to the chromatographic method as; the flow rate 1.5 ± 0.1 mL/min, temperature 35 °C ± 2 °C, and the ratio of acetonitrile in the mobile phase ± 2%, followed by calculating the %RSD.

### 2.8. Preparation of CSPE loaded lipid nanoparticles (CSPE-LNPs)

Preparation of CSPE-LNPs was done using high shear homogenization - ultrasonication technique following [14] with some modifications. Briefly, heating of the oily phase of CSPE-SLN (composed of cocoa butter) and CSPE-NLC (composed of cocoa butter/ olive oil) was done reaching a temperature exceeding the melting point of the lipids. Consequently, preparation of the aqueous phase of both CSPE-SLN and CSPE-NLC was achieved by dissolving tween 80 in distilled water followed by heating to the same temperature of the oil phase. At that particular stage, dissolving a certain weight of the CSPE that contains a known concentration of the active component hesperidin in the aqueous phase was performed. Correspondingly, addition the aqueous phase to the oily phase and homogenization using different homogenization speed for 10 min was done. Following this, the resulting coarse emulsion is sonicated for 10 min using Branson Sonifier ® 450 (CT, USA) to prevent the process of agglomeration during cooling. After sonication, nanoparticles were formed by congealing the sonicated dispersions for 2 h at 4 °C.

#### 2.8.1. Design of LNPs experiments

Evaluating the effect of individual and joined different formulation variables on CSPE-SLN and CSPE-NLC performance and characteristics were achieved through a $2^3$ full factorial design. [15]. The effect of hesperidin concentration ($X_1$), homogenization speed ($X_2$), and nanoparticle type($X_3$) as independent variables was evaluated on three dependent variables, the particle size of CSPE-LNPs ($Y_1$), entrapment efficiency ($Y_2$), and occlusion effect ($Y_3$). The independent variables were optimized using Design Expert 7.0 software (State-Ease Inc., USA) at two different levels: low (−1) and high (+1) (Table 1). The actual levels of variables (Table 1) were selected based on the preliminary experiments (data not shown).

First-order polynomial regression equations were created between the coded independent factors and responses(Y). The polynomial equations can be employed to conclude after considering the magnitude of the coefficient and the mathematical sign it carries. With numeric factors ($X_1$ and $X_2$), a positive sign in front of the terms indicates a synergistic effect while a negative sign indicates the antagonistic effect of the factors. While in case of the categoric factor ($X_3$); the positive sign

**Table 1**
Formulation of CSPE loaded lipid nanoparticles (CSPE-LNPs) based on $2^3$ factorial design.

| Formulation Code | Normalized level of the independent variables | | |
|---|---|---|---|
| | CSPE amount ($X_1$) | Homogenization Speed ($X_2$) | Nano-lipid types ($X_3$) |
| **F1** | **-1** | **+ 1** | **SLNs** |
| **F2** | **+ 1** | **-1** | **SLNs** |
| **F3** | **+ 1** | **+ 1** | **SLNs** |
| **F4** | **-1** | **-1** | **SLNs** |
| **F5** | **-1** | **+ 1** | **NLCs** |
| **F6** | **+ 1** | **-1** | **NLCs** |
| **F7** | **+ 1** | **+ 1** | **NLCs** |
| **F8** | **-1** | **-1** | **NLCs** |

**(Actual values of the independent variables: $X_1$, +1 = 1000 mg, −1 = 500 mg; $X_2$, +1 = 20000 rpm, −1 = 15000 rpm; $X_3$, +1 = SLNs, −1 = NLCs).**

indicates its presence and the negative sign means its absence. The model term is considered significant if the *p*-value was $< 0.05$ as stated by One-way ANOVA.

### 2.9. Characterization of the prepared CSPE-LNPs

#### 2.9.1. Particle size, polydispersity index (PDI) and zeta potential measurements

A zeta-seizer (Malvern Instruments Ltd) was used to achieve a total confirmation of the nanometric size of the prepared formulae as well as their dispersed nature and stability, particle size (Z-average), polydispersity index (PDI), and zeta potential (mV).that was done at a temperature of at 25 °C. Dilution of the aqueous CSPE-SLN and CSPE-NLC dispersions with distilled water before analysis was done aiming to achieve optimal kilo counts per second (kcps) of 50–200 for measurements [16]. The recorded results found in (Table 2) represent the means ± standard deviations (SD) of three determinations.

#### 2.9.2. Transmission electron microscopy

Examination of the morphological structure of the CSPE-SLN and CSPE-NLC was done using transmission electron microscopy (TEM) (CM12 Philips, Amsterdam, Netherlands) Table 3.

#### 2.9.3. Occlusion test

For evaluation of the occlusive effect of CSPE-SLN and CSPE-NLC, a modified in vitro occlusion test was employed. In this test, beakers were filled with 30 g of water and covered with Whatman® filter paper grade 42 (Sigma-Aldrich, USA). 300 µl of CSEP-SLN and CSPE- NLC samples were spread on the filter surface. Following this, using a beaker covered with filter paper spread with water as a reference was done. Further, the storage of beakers at 32°C to mimic the temperature of the skin surface and weighing at 0, 6, 24, and 48 h was done. The aim behind that was to calculate water evaporation through the filter paper in terms of water loss [14]. The occlusion factor (F) was calculated in three replicates (n = 3) at 6, 24, and 48 h using the following Equation:

$$F = \frac{R - S}{R} \times 100$$

where R = reference water loss and S = water loss with the sample. An F value equals 0 indicates the absence of occlusive effect while an F value equals 100 indicates maximum occlusive property. To confirm the formation of the occlusive film on the filter paper, visualization of filter paper by scanning electron microscopy (SEM) was performed at the end of the experiment.

#### 2.9.4. Entrapment efficiency (EE)

Determination of EE (%) of different CSE-LNPs formulations was achieved by analyzing the concentration of free hesperidin in 1 mL of dispersion medium after being diluted with water at a certain rate. The mixture was exposed to centrifugation at 16,000 rpm for 30 min at 15 $^0$C, then filtration through a disk filter (pore size: 0.45 µm) was done. Finally, determination of the amount of hesperidin in each supernatant (free drug) was done by the use of a novel developed and validated HPLC analytical method [17].

The Entrapment efficiency (%EE) was determined using the following equation:

$$EE\% = \frac{Winitialdrug - Wfreedrug}{Winitialdrug} \times 100$$

Where $W_{\text{initial drug}}$ is the amount of either SP or PG added in the formulation and $W_{\text{free drug}}$ is the amount of each drug in the supernatant [18].

### 2.10. Preparation of CSPE-LNPs cream

Selection of the optimized CSPE-LNPs formula to be formulated as a topical anti-aging cream was done [19], using stearic acid as a lipid phase. Packaging of the final anti-aging product was performed in a tightly closed container for further investigation.

#### 2.10.1. Hesperidin content of CSPE-LNPs based cream

In order to determine hesperidin content in the prepared cream, weighing 1 g of CSPE-LNPs based anti-aging cream in a 10 mL volumetric flask was done followed by, dissolving it in 5 mL of methanol [20]. The next step was adjusting the samples to 10 mL volume with methanol and mixing them thoroughly, followed by being filtered using 0.45 µ membrane filter, and being analyzed using the previously mentioned HPLC analytical method.

#### 2.10.2. In- vitro drug release study

Dialysis method was employed to measure the in-vitro release profiles of CSPE-LNPs based cream. Typically, 2 g (equivalent to a known amount of Hesperidin) of pure CSPE -based cream and CSPE-LNPs based cream each was placed in two different dialysis tubes (15,000 Mw cut-offs). That was done after being soaked in deionized water for 12 h. The dialysis tubes were then immersed in a vessel containing 100 mL of pH 6.8 phosphate buffer saline (PBS), at a temperature of 37 ± 0.5 °C and stirred at 100 rpm. Samples were collected at various time intervals and instantly replaced with fresh dissolution medium. Samples were filtered using disk filter paper (0.45 µm), the concentration of hesperidin was determined using HPLC method described previously [21].

### 2.11. The in vivo antiwrinkle study

#### 2.11.1. Experimental animals

48 Adult female Swiss Albino mice weighing 25–30 g were obtained from the National Scientific Research Centre in Giza, Egypt. They had unrestricted access to food and water and were acclimatized for 7 days before commencing with the experimentation. All experiments were conducted after the approval of the ethics committee at October University for Modern Sciences and Arts (MSA) and per the guidelines set by

**Table 2**
Observed values of responses for 8 formulations of *CSPE* extract loaded lipid nanoparticles (CSPE-LNPs).

| Formula code | Observed responses | | | | |
|---|---|---|---|---|---|
| | ($Y_1$) Particle size* (nm) | PDI* | Zeta potential* (mv) | ($Y_2$) Entrapment efficiency* (%) | ($Y_3$) Occlusion effect* (%) |
| F1 | 237.8 ± 9.2 | 0.445 ± 0.01 | -26.1 ± 3.1 | 84.15 ± 3.5 | 24.45 ± 1.2 |
| F2 | 347.5 ± 15.3 | 0.772 ± 0.08 | -26.4 ± 2.2 | 80.45 ± 4.1 | 34.08 ± 1.9 |
| F3 | 255.3 ± 7.5 | 0.448 ± 0.11 | -26.2 ± 1.3 | 93.50 ± 3.3 | 29.11 ± 3.1 |
| F4 | 476.9 ± 17.1 | 0.787 ± 0.021 | -26.7 ± 4.1 | 90.10 ± 2.4 | 35.1 ± 3.5 |
| F5 | 294.6 ± 16.9 | 0.435 ± 0.04 | -24.9 ± 3.5 | 90.16 ± 5.1 | 42.52 ± 2.3 |
| F6 | 322.7 ± 8.7 | 0.645 ± 0.072 | -33 ± 4.6 | 85.75 ± 5.2 | 10.79 ± 1.4 |
| F7 | 243.3 ± 12.5 | 0.444 ± 0.034 | -25.2 ± 1.4 | 97.23 ± 2.3 | 60.45 ± 5.2 |
| F8 | 301.6 ± 14.6 | 0.415 ± 0.022 | -26.7 ± 2.3 | 91.8 ± 2.2 | 31.16 ± 3.1 |

Note: *Results are expressed as the mean of three replicates ± SD.
Abbreviation: PDI, polydispersity index.

**Table 3**
Statistical analysis results (ANOVA) for the dependent responses.

| | Particle Size (nm, $Y_1$) | | | EE % ($Y_2$) | | | Occlusion effect ($Y_3$) | | |
|---|---|---|---|---|---|---|---|---|---|
| Source | Sum of Squares | Mean Of Square | p-value | Sum of Squares | Mean Of Square | p-value | Sum of Squares | Mean Of Square | p-value |
| **A** | 36185.55 | 36185.55 | < 0.0001 | 85.93 | 85.93 | < 0.0001 | 509.07 | 509.07 | < 0.0001 |
| **B** | 296.70 | 296.70 | 0.4206 | 250.75 | 250.75 | < 0.0001 | 485.65 | 485.65 | < 0.0001 |
| **C** | 9628.52 | 9628.52 | 0.0013 | 60.30 | 60.30 | < 0.0001 | 112.31 | 112.31 | < 0.0001 |
| **AB** | 7766.02 | 7766.02 | 0.0025 | 0.53 | 0.53 | 0.3398 | 0.15 | 0.15 | 0.7484 |
| **AC** | 10185.86 | 10185.86 | 0.0011 | 1.225E- 003 | 1.225E-003 | 0.9619 | 1516.13 | 1516.13 | < 0.0001 |
| **BC** | 8086.51 | 8086.51 | 0.0022 | 6.10 | 6.10 | 0.0101 | 248.77 | 248.77 | < 0.0001 |
| **Residual** | 3293.12 | 411.64 | | 3.51 | 0.50 | | 10.90 | 1.36 | |
| **Model** | 72149.14 | 12024.86 | < 0.0001 | 403.61 | 57.66 | < 0.0001 | 2872.08 | 478.68 | < 0.0001 |
| R-Squared | 0.9563 | | | 0.9914 | | | 0.9962 | | |
| Adj R-Squared | 0.9236 | | | 0.9828 | | | 0.9934 | | |
| Pred R-Squared | 0.8254 | | | 0.9550 | | | 0.9849 | | |
| Adeq Precision | 16.773 | | | 35.228 | | | 62.932 | | |

A- CSPE concentration, B-Homogenization speed, C-Nano-lipid types.

the National Institute for Health Guide for the care and treatment of laboratory animals (Ethics form no. PH3/EC3/2018PD).

*2.11.2. Experimental design*

The present study aims at examining the effect of a nano-formulation of CSP on photoaging induced by UV exposure in mice.

Mice were randomly allocated into six groups eight mice per each group.

1. The control group, which was the normal non-UV-irradiated group.
2. The UV group, which was the injured UV-irradiated non treated group.
3. The standard group, which was UV-irradiated and treated with the standard marketed cream (C-topic).
4. The CSPE- NLC formulation group, which was UV-irradiated and treated with the test formula under investigation.
5. The plain cream group, which was UV-irradiated and treated with only a plain cream base.
6. The pure CSPE cream group, which was UV-irradiated and treated with pure CSPE in a cream base.

*2.11.3. Induction of wrinkles and treatment*

A hair removal cream (for sensitive skin) was used to remove the fur off the back of mice, and the cream was preferred over shaving to avoid any injury or trauma that might occur due to the shaving blade [22]. Photoaging was induced by UV radiation, where the UV lamp was placed 30 cm above the dorsal skin of the mice and the minimal erythemal dose (MED) was determined by exposing the skin to several different doses of UV radiation and detecting the formation of erythema after 24 hr. Wrinkles and photoaging were induced by exposing the dorsal skin to 1MED (100 mJ/cm$^2$) three times weekly for six weeks [23,24].

Topical treatments were initiated after the induction of wrinkles where 0.25 gm of each formula was applied twice daily for five weeks to the designated group [25].

At the end of the experiment, photoaging was assessed macroscopically by photographing the dorsal skin right.

*2.11.4. Tissue collection and biochemical analysis*

After euthanization, the collected skin samples (measuring 4 mm) were homogenized in 1.5 mL extraction buffer (containing 10 mM Tris pH 7.4, 150 mM NaCl, 1% Triton X-100) per gram of tissue utilizing a glass homogenizer (Biospec Product, mini-BeadBeater-8), the incubated mixture was placed on ice and sonicated for 20–30 s then centrifuged at 5000 rpm at 15 min and the supernatant collected for measurement of collagen type I (CUSABIO, China), Catalogue no. CSB-E01124r, Cyclooxygenase-2 activity (COX-II) (mmuno-Biological Laboratories Co., Ltd, Japan), Catalogue no. 38511, Elastin (Wuhan Fine Biological Technology Co., Ltd, China), Catalogue no. ER0571, Prostaglandin E2 (Elabscience Biotechnology Co.,Ltd, USA), Catalogue no. E-EL-R0107, C-Jun N-Terminal Kinases (JNK) (Elabscience Biotechnology Co.,Ltd, USA), Catalogue no. E-EL-R0305 using the rat enzyme immunoassay kits and Malondialdehyde (MDA), and Superoxide dismutase (SOD) (Biodiagnostic, Diagnostic and research reagents, Egypt) using the colorimetric method according to manufactured instructions.

GraphPad Prism version 6 was used for analyzing the parameters. All data were presented as the mean ± SD. One-way analysis of variance (ANOVA) followed by Tukey Kramer multiple comparisons tests were used to perform comparisons between groups. The student *t*-test was used to compare two groups, $P < 0.05$ was the accepted significance level.

*2.11.5. Gene expression and qRT-PCR*

Matrix metalloproteinase 1 (MMP1) RNA was extracted from tissues using a TRIzol RNA mini kit Cat. No. 15596-026 (Invitrogen, Carlsbad, CA), the extracted RNA was eluted in 40 μl of nuclease-free distilled water.

The RNA of each sample was reverse transcribed the SuperScript First-Strand Synthesis Kit (Invitrogen, Carlsbad, CA, USA), quantification of MMP1 PCR was carried out by using of MMP1 PCR fluorescence quantitative diagnostic kit Cat. No. (A.S 5127302) with a Stratagene Mx3000P (Agilent Technologies, Germany).

The primers were purchased from Qiagen PCR array who possesses the proprietary information of the primer sequences. Thermal cycling and fluorescence detection were performed using a Rotor-Gene Q5 plex real-time Rotary analyzer (Corbettlife Science, USA).

## 3. Results

### 3.1. Identification of CSPE major metabolites via HPLC-QToF-MS-MS

A total of twenty-nine metabolites were tentatively characterized in CSPE via HPLC-QToF-MS-MS analysis in the positive mode. The peak assignments were based on their molecular and fragment ions, molecular formulae, and retention times as compared to data from MarkerView1.3, Sciex® library, and available literature. The metabolites were grouped according to their chemical classes, namely; flavonols, flavones, isoflavones, flavanones, coumarins, phenolic compounds, and phenolic acids as presented in Table 4.

### 3.2. In vitro evaluation of CSPE antioxidant activity via ORAC assay

The antioxidant activity of CSPE was evaluated via the ORAC in vitro assay. CSPE possessed a good antioxidant activity with $ED_{50}$ of (30.12 ± 3.59 μg/mL) which is close to the used standard Trolox with $ED_{50}$ of (27.0 ± 13.41 μg/mL). CSPE showed a DPPH inhibitory activity with an $ED_{50}$ value of (32.22 ± 3.13 μg/mL) compared to ascorbic acid with an $ED_{50}$ value of (1.83 ± 1.41 μg/mL).

**Table 4**
Tentative characterization of CSPE metabolites via HPLC-QToF-MS-MS analysis.

| No. | Molecular weight | Molecular formula | $[M+H]^-$ | Fragments ($MS^n$) | Identification | Reference |
|---|---|---|---|---|---|---|
| **Flavonols** | | | | | | |
| 1 | 448.1077 | $C_{21}H_{20}O_{11}$ | 449.1077 | 449.11, 304.05, **303.10**, 288.10, 287.06, 274.05, 270.10, 254.10, 245.05, 229.05, 165.02, 153.02, 129.05, 128.10, 85.10, 71.05, 70.10 | Quercetin-3-*O*- rhamnoside (Quercitrin) | [61] |
| 2 | 464.103 | $C_{21}H_{20}O_{12}$ | 465.103 | 465.10, 304.06, **303.05**, 302.04, 301.10, 300.10, 273.04, 272.10, 257.05, 229.05, 153.02, 121.03, 91.04, 61.03, 60.10 | Quercetin − 3-*O*-galactoside (Hyperoside) | [61] |
| 3 | 464.103 | $C_{21}H_{20}O_{12}$ | 465.103 | 465.10, 304.05, **303.10**, 302.04, 301.10, 300.10, 273.04, 272.10, 257.04, 243.10, 229.05, 153.02, 111.01 | Quercetin-3-*O*- glucoside (Isoquercitrin) | [62] |
| 4 | 464.103 | $C_{21}H_{20}O_{12}$ | 465.103 | 465.10, 304.05, **303.05**, 302.10, 301.10, 300.10, 229.05, 183.04, 179.10, 163.04, 153.02, 150.10, 121.03, 111.01 | Quercetin-4′-glucoside (Spiraeoside) | [63] |
| 5 | 610.1603 | $C_{27}H_{30}O_{16}$ | 611.1603 | 611.16, 465.10, 449.11, 304.05, **303.05**, 301.03, 274.04, 273.04, 153.02 | Quercetin-3-*O*-glucosyl-7-*O*-rhamnoside | [64] |
| 6 | 610.1603 | $C_{27}H_{30}O_{16}$ | 611.1603 | 611.16, 551.08, 505.50, 465.10, 385.47, 364.52, **303.74**, 302.11, 301.02, 300.02, 274.05, 273.04, 272.03, 245.04, 213.88, 187.03 | Quercetin-3-*O*-rutinoside (Rutin) | [65] |
| 7 | 432.1154 | $C_{21}H_{20}O_{10}$ | 433.1154 | 433.12, **287.12**, 229.12 | Kaempferol-7-*O*-rhamnoside | [66] |
| 8 | 578.1709 | $C_{27}H_{30}O_{14}$ | 579.1709 | 579.17, 435.16, 434.16, 432.11, 430.16, 429.16, 428.16, 288.06, 286.05, 285.04, 129.16 | Kaempferol-3,7-*O*-di-rhamnoside | [67] |
| 9 | 478.1193 | $C_{22}H_{22}O_{12}$ | 479.1193 | 479.11, **317.07, 316.06**, 313.11, 301.04, 288.06, 285.04, **273.04**, 272.03, 259.07, 245.04, 244.04, 153.02, 145.11, 127.11 | Isorhamnetin-3-*O*-glucoside | [68] |
| 10 | 610.1608 | $C_{27}H_{30}O_{16}$ | 611.1608 | 611.16, 353.15, 287.15 | Luteolin 6,8-di-*C*-glucoside (Lucenin-2) | [68] |
| 11 | 564.1562 | $C_{26}H_{28}O_{14}$ | 565.1562 | 565.16, 379.15, 337.15, 313.15 | Apigenin-*O*,*C*-pentosyl-hexoside | [69] |
| 12 | 594.1659 | $C_{27}H_{30}O_{15}$ | 595.1661 | **595.17**, 559.16, 481.16, 457.16, 439.16, 379.16, 325.16, 307.16 | Apigenin 6,8-di-*C*-glucoside (Vicenin-2) | [68] |
| 13 | 432.1134 | $C_{21}H_{20}O_{10}$ | 433.1056 | 433.11, 397.10, 396.11, 379.09, 343.09, 342.11, 337.07, 336.11, 322.11, 314.11, **313.07**, 296.11, 295.06, 285.08, 284.07, **283.06**, 282.11, 256.08, 121.03 | Apigenin-8-*C*-glucoside (Vitexin) | [70] |
| 14 | 432.1131 | $C_{21}H_{20}O_{10}$ | 433.1131 | 433.11, **313.11, 283.11** | Apigenin-6-*C* glucoside (Isovitexin) | [65] |
| 15 | 594.1659 | $C_{27}H_{30}O_{15}$ | 595.1659 | 595.17, 577.16, **413.12**, 379.16, 378.16, 368.16, 359.09, 349.16, 348.16, 336.16, 329.06, 314.16, 312.16, 311.16, 284.16 | Isovitexin-2″-*O*-glucoside | [67] |
| 16 | 432.1134 | $C_{21}H_{20}O_{10}$ | 433.1134 | 433.11, 272.11, **271.06, 268.11**, 267.11, 242.06, 153.02 | Apigenin-7-*O*-glucoside (Cynaroside) | [71] |
| 17 | 578.1713 | $C_{27}H_{30}O_{14}$ | 579.1713 | 597.17, 272.16, **271.16, 269.16**, 268.16, 270.16, 269.16, 268.16, 267.16 | Apigenin 7-*O*-neohesperidoside (Rhoifolin) | [65] |
| 18 | 608.1819 | $C_{28}H_{32}O_{15}$ | 609.1819 | 609.18, 302.17, **301.07**, 300.17, **286.05**, 285.17, 284.17 | Diosmetin 7-neohesperido-side (Neodiosmin) | [68] |
| 19 | 328.1026 | $C_{18}H_{16}O_6$ | 329.1026 | 329.10, **314.45**, 295.06, 283.62, 269.04, 267.06, 255.05, 248.49, 243.06, 229.09, 225.05, **200.04**, 185.06, 183.88, 172.05, 168.08, 119.05, 118.04 | 5-Hydroxy-3′,4′,5′-trimethoxyflavone | [72] |
| **Isoflavone** | | | | | | |
| 20 | 432.1134 | $C_{21}H_{20}O_{10}$ | 433.1134 | 433.11, 361.11, 343.08, 325.08, 313.07, 295.06, 285.07, 284.06, 283.07, **271.06,** 269.60, 256.07, 253.05, 242.06, 241.09, 228.04, 226.09 | Genistein β-glucoside (Sophoricoside) | [73] |
| **Flavanones** | | | | | | |
| 21 | 610.1971 | $C_{28}H_{34}O_{15}$ | 611.1971 | 611.20, 593.19, 575.19, 557.19, 490.35, 489.19, 465.13, **449.15**, 447.13, 431.14, 413.12, 395.10, 369.10, 345.10, 334.99, 327.09, 315.09, 313.06, 305.09, **303.59**, 302.19, 300.19, 294.05, 289.07, 288.25, 285.08, 281.69, 281.06, 271.05, 269.04, 263.05, 260.06, 245.05, 244.07, 243.07 | Hesperetin-7-rutinoside (Hesperidin) | [68] |
| 22 | 434.1292 | $C_{21}H_{22}O_{10}$ | 435.1292 | 435.13, 274.12, **273.12**, 270.12, 179.03, **153.02**, 146.12, 123.05, 91.05, 67.02 | Naringenin-7-*O*-glucoside (Prunin) | [74] |
| **Coumarin** | | | | | | |
| 23 | 276.0997 | $C_{15}H_{16}O_5$ | 277.0997 | 277.11, 217.46, 212.63, **209.04, 208.10,** 207.03, 202.49, 194.11, 181.05, 179.03, 165.64, 163.04, 139.48, 138.03, 135.04, 121.06, 119.14, 115.86, 113.31, **109.03,** 106.90 | Capensine | [66] |
| **Phenolic compounds and phenolic acids** | | | | | | |
| 24 | 390.1393 | $C_{20}H_{22}O_8$ | 391.1393 | 391.14, 285.10, 269.07, 231.10, 147.06, 137.06, 121.06, 113.06, 97.06 | Resveratrol 3-*O*-glucoside | [75] |
| 25 | 274.0841 | $C_{15}H_{14}O_5$ | 275.0841 | 275.09, 235.35, 229.09, 187.53, 170.07, **169.09**, 166.02, 163.07, 159.08, 153.06, 147.04, 145.07, 144.12, 139.04, 135.08, 132.05, 127.04, **125.16**, 123.05, 122.04, 121.10, 111.05, 109.03, **107.05** | Phloeritin | [76] |
| 26 | 354.1029 | $C_{16}H_{18}O_9$ | 355.1029 | 355.10, **193.21**, 163.10 | Chlorogenic acid | [70] |
| 27 | 354.1029 | $C_{16}H_{18}O_9$ | 355.1029 | 355.10, **193.11**, 116.70, 94.61, 86.71, 60.21 | 3-Caffeoylquinic acid | [77] |
| 28 | 530.1522 | $C_{26}H_{26}O_{12}$ | 531.1522 | 531.15, **369.12, 193.11, 176.80**, 174.81, 136.91, 135.71 | Feruloyl-caffeoyl-quinic acid | [72] |
| 29 | 368.1179 | $C_{17}H_{20}O_9$ | 369.1179 | 369.12, **194.71**, **136.13,** 135.71, 118.81 | Feruloylquinic acid | [78] |

### *3.3. In vitro evaluation of CSPE anti-elastase and anti-collagenase activities*

CSPE was screened for its in vitro inhibitory activities of elastase and collagenase enzymes, the extract inhibited the elastase enzyme with an $IC_{50}$ value of (299.04 μg/mL) and the collagenase enzyme with an $IC_{50}$ value of (188.61 μg/mL). The result showed that CSPE has promising anti-elastase and anti-collagenase activities with comparable $IC_{50}$ values the tested standards Elafin as anti-elastase ($IC_{50}$ = 250.09 μg/mL) and epigallocatechin gallate (EGCG) as anti-collagenase ($IC_{50}$ = 112.12 μg/mL).

### 3.4. HPLC standardization of the extract

The HPLC chromatogram of the extract displayed that hesperidin was the major component (Fig. 1A) and was eluted at 24.034 which is the same retention time of standard hesperidin as revealed from its chromatogram (Fig. 1B). The extract was standardized to comprise hesperidin of not less than 15.53 ± 0.152 mg%. The chromatographic method was validated as per the ICH recommendations [26]. Regarding the linearity and range; the adjusted chromatographic conditions were set, then, the linearity of hesperidin was identified via examining different concentrations in triplicate analysis. Hesperidin calibration curve exhibited a linear correlation between peak area and equivalent concentration within the concentrations of 10–200 μg/mL with a correlation coefficient of 0.9995, additionally, all parameters of the regression equation were computed as demonstrated in (Fig. 1C). As for the accuracy of the method; it was ascertained as the mean Recovery % ± SD of the three investigated concentrations (40, 80, 160 μg/mL) was 100.83 ± 1.33. The accuracy was further assessed by performing a statistical comparison between the results obtained from analyzing hesperidin standard material by the developed method and those of a

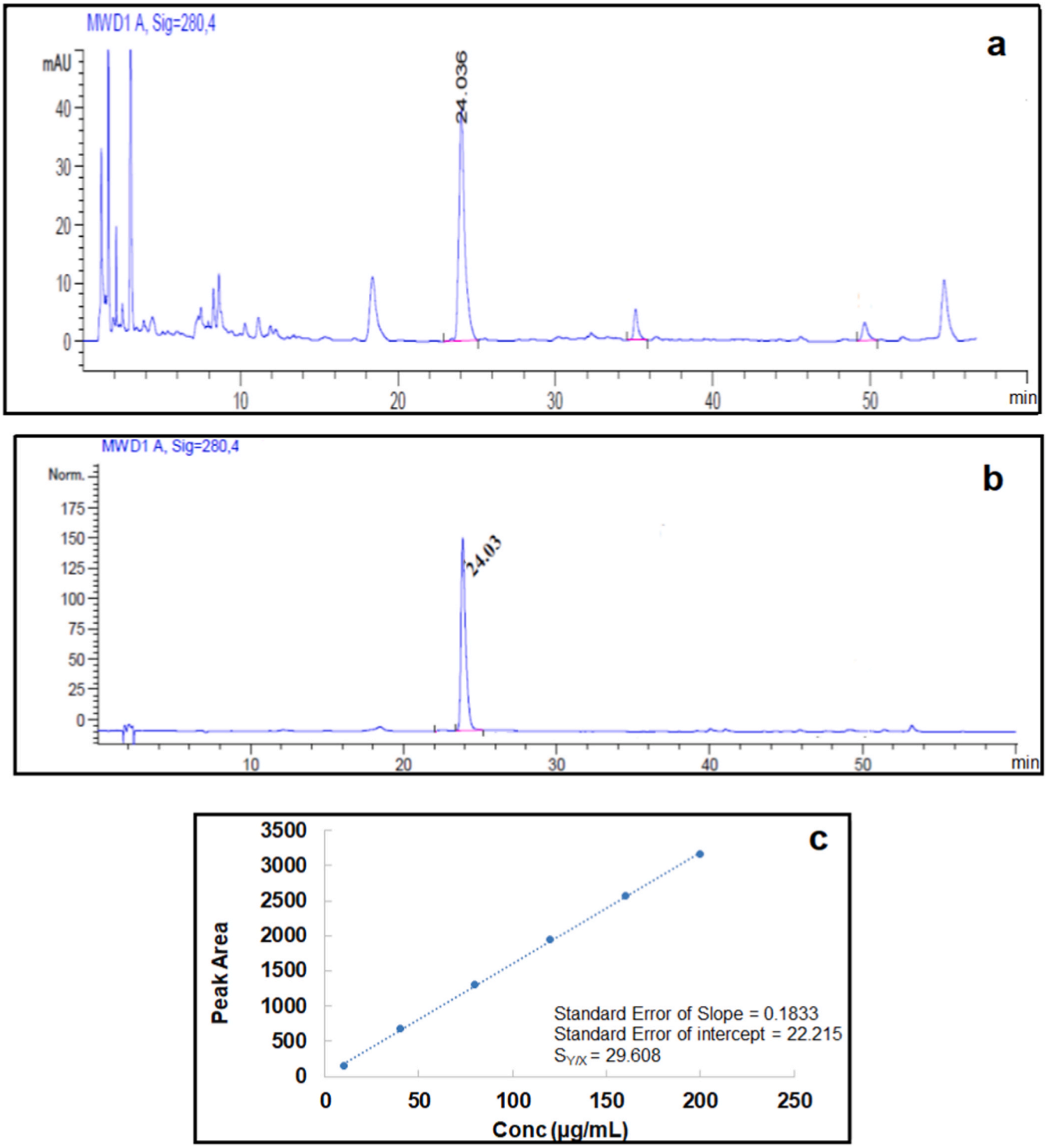


**Fig. 1.** a- HPLC chromatogram of the extract, b- HPLC chromatogram of standard hesperidin and c- Calibration curve of standard hesperidin.

reported method [27], where both Student's *t*-test and Variance ratio F test assured the absence of any significant difference between the performances of both methods (Table 5). Regarding the precision; it was assured as the % RSD of the same three concentrations was 1.73 and 1.92 for intraday and inter-day analysis, respectively. The robustness of the method was apparent from the calculated %RSD which was found to be 2.89, 1.56, and 2.34 for the intended changes in flow rate, temperature, and acetonitrile ratio, respectively. The method was also proved to be selective as the chromatogram of pure ethanol showed no peaks at 24.034 min when measured at 280 nm.

Even though it is a traditional practice during the development of an HPLC method to consider its proper validation, it is also important to consider the greenness evaluation of the method including the extract preparation step to judge its safety on health and environment. Consequently, three assessment tools were utilized to judge the greenness of the developed HPLC method; National Environmental Methods Index (NEMI) [28], Analytical Eco-Scale [29], and Green Analytical Procedure Index (GAPI) [30], where the results of this assessment are demonstrated in (Table 5). Concerning NEMI tool; it revealed two green quadrants reflecting that the used reagents are not persistent, bioaccumulative, or toxic and that the method is not corrosive as the pH of the medium was in the pH range from 2 to 12, however, two unshaded quadrants were reflecting that the solvents are hazardous and that the produced waste was more than 50 mL (Table 5). A more detailed and quantitative assessment tool was also utilized which is the Analytical Eco-Scale. This tool considers that a method is ideal green when it achieves a score of 100, penalty points are then subtracted from the 100 scores reflecting the amount of materials, hazards, energy, and waste that are generated by the method. Upon applying the Analytical Eco-Scale rules; the developed method including the extract preparation step has collected a score of 66 (Table 5) which implies that it is an acceptable green method. Lastly, the GAPI assessment tool was used for the greenness evaluation of the method. GAPI utilizes five pentagrams to judge the influence of the analytical method on the environment with the aid of a color-coding; green, yellow, and red signifying low, medium, and high environmental influence, respectively. As displayed in (Table 5), the GAPI evaluation of the developed method reflected its medium impact on the environment as the majority of the fields were

**Table 5**
Statistical Comparison between the results of the developed and reported [2] methods for the determination of standard hesperidin and the greenness evaluation of the chromatographic method by NEMI, Analytical Eco-scale and GAPI tools.

| Statistical comparison between the developed and reported methods | | | | |
|---|---|---|---|---|
| Item | Developed Method | | Reported method[b] | |
| **Mean**[a] | 100.29 | | 99.37 | |
| **SD** | 0.90 | | 0.87 | |
| **Variance** | 0.8036 | | 0.7644 | |
| **N** | 6 | | 5 | |
| **Student's *t*-test**[c] | 1.709 (2.2621) | | | |
| **F value**[c] | 1.051 (6.2561) | | | |
| **Greenness evaluation of the developed method** | | | | |
| | **Analytical Eco-Scale** | **Penalty points (pp)** | **NEMI Pictogram** | **GAPI Assessment** |
| **Reagents** | Ethanol | 8 | 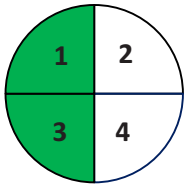 | 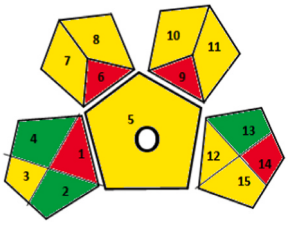 |
| | Formic acid | 4 | | |
| | Acetonitrile | 8 | | |
| | Methanol | 6 | | |
| **Instruments** | LC-UV $\leq$ *1.5 KWh/sample* | 1 | | |
| | Occupational hazards | 0 | | |
| | Rotavap | 1 | | |
| | Sonicator | 1 | | |
| | Waste | 5 | | |
| **Total pp** | | **34** | | |
| **Eco-Scale** | | **66** | | |
| **Interpretation of NEMI and GAPI** | | | 1. Not PPT reagents (Green)<br>2. Hazardous solvents (Not green shaded)<br>3. Not corrosive method (Green)<br>4. Waste > 50 mL (Not green shaded) | Sample preparation (1–8)<br>1. Sample collection: Off-line (Red)<br>2. Sample preservation: None (Green)<br>3. Sample transport: required (Yellow)<br>4. Sample storage: None (Green)<br>5. Type of method: Simple procedure is used for sample preparation (Yellow)<br>6. Scale of extraction: Macro-extraction (Red)<br>7. Solvents for sample preparation: green solvents (Yellow)<br>8. Additional treatment: Solvent removal (Yellow)<br>**Reagents and solvents (9–11)**<br>9. Amount: > 100 mL (Red)<br>10. Health hazard: Moderately toxic (Yellow)<br>11. Safety hazard: Highest NFPA = 3 (Yellow) NFPA (National Fire Protection Association)<br>**Instrumentation (12–15)**<br>12. Energy: $\leq$ 1.5 KWh/sample (Yellow)<br>13. Occupational hazard: None (Green)<br>14. Waste: > 10 mL (Red)<br>15. Waste treatment: Degradation (Yellow)<br>16. **Circle in the middle of GAPI**: Procedure is used for quantification |

[a] Average of three experiments.
[b] The reported method is an HPLC method using RP18 column, a mixture of methanol–water (60:40, v/v) as a mobile phase in an isocratic mode at a flow rate of 1.5 mL/min and UV detection at 345 nm.
[c] The corresponding tabulated t and F values at p = 0.05.

yellow color-coded.

### 3.5. Preparation of Citrus sinensis peel extract loaded lipid nanoparticles (CSPE-LNPs)

Preparation of the CSPE-LNPs formulae from completely natural components (active ingredient Hesperidin + lipid carriers) was successfully done. That was achieved by the homogenization ultrasonication technique. The selection of this method was intended to comply with the natural theme of this study as one of its merits the absence of organic solvents [31].

#### 3.5.1. Characterization of the prepared CSPE-LNPs

Evaluation of eight different formulae of CSPE-LNPs was done for their particle size ($Y_1$), PDI, zeta potential, EE % ($Y_2$), and occlusion effect % ($Y_3$) as shown in Table 2. The mean particle size ($Y_1$) ranged from 237.8 ± 9.2–476.9 ± 17 nm depending on the variables' level selected during production as displayed in Table 2. PDI values ranged from 0.415 ± 0.022–0.787 ± 0.021 where all formulae showed accepted homogeneity as confirmed in the morphological examination. Transmission electron microscopy (TEM) (Fig. 2) confirmed that all particles were spherical and homogeneous with no evidence of aggregates. Furthermore, all formulae exhibited negative zeta potential. While EE% ($Y_2$) was in the range of 84.15 ± 3.5% to 97.23 ± 2.3% due to the variation in factors combination. Moreover, the Occlusion effect ($Y_3$) ranged from 10.79 ± 1.4% to 60.45 ± 5.2% as shown in Table 2.

#### 3.5.2. Mathematical modeling and statistical analysis of the experimental data by Design Expert Software

Besides, analysis of responses values ($Y_1$ to $Y_3$) of the formulations of CSPE-LNPs was performed employing Design Expert 7.0.0 software and mathematical Eqs. 1 to 3 were built up to identify and quantify the effect of formulation variables ($X_1$, $X_2$, $X_3$) on each response parameter.

The equation in terms of coded factors:

**Particle size ($Y_1$)** = 318·18 + 47·56 A - 4·31 B + 24·53 C + 22·03 AB + 25·23 AC + 22·48 BC (1)

(Where F=29.21, $P < 0.05$, $R^2 = 0.9996$).

**Entrapment efficiency ($Y_2$)** = 90·25–2·3175 A - 3·95875 B - 1·94125 C - 0·18AB + 8·74 AC + 0.6175 BCE + 0.025 ABC (2)

(Where F = 115.10, $P < 0.05$, $R^2 = 0.9550$).

**Occlusion effect ($Y_3$)** = 34·60 – 5·64 A + 5·51 B – 2·65 C - 0.097 AB + 9·73 AC −3·94 BCE – 0.79 ABC (3)

(Where F = 351.41, $P < 0.0500$, $R^2 = 0.9997$)Where A, B, and C are the coded levels of the independent variables $X_1$ (Hesperidin concentration), $X_2$ (homogenization speed) $X_3$ (Nanoparticles type) respectively. The interactions (AB), (AC) and (BC) express how the response changes on the interaction of the two factors studied. While (K) is a constant value which is the arithmetic mean response of the formulations. The influence of the factor is considered significant if the p-value < 0.05 as stated by ANOVA. Table 3 showed the statistical analysis results (ANOVA) for the responses of particle size ($Y_1$), EE ($Y_2$), and occlusion effect ($Y_3$). It is obvious that from Table 3, all chosen independent variables ($X_1$, $X_2$, and $X_3$) have a significant effect on the investigated responses namely entrapment efficiency ($Y_2$) and occlusion effect ($Y_3$) with p-value < 0.05. While the particle size response ($Y_1$) has been significantly affected by the independent variables ($X_1$ and $X_3$) only (Fig. 3).

High $R^2$ values indicated good agreement between formulation variables and response parameters. Additionally, the model of each response was significant with p-value < 0.05(Table 3). Adequate Precision is used to determine the signal to noise ratio. A ratio of more than 4 is desirable. The present model shows a reasonable signal; therefore, this model can be used to navigate the design space.

#### 3.5.3. Selection of optimized formulation

The software Design Expert 7.0.0 suggested CSPE-NLC (F7) as optimized formula obtained by applying our constraints of minimize particle size, maximize entrapment efficiency, maximize occlusion effect and with good desirability (which has highest desirability reach 1).

#### 3.5.4. Release study of CSPE- NLC based cream

The performance of in vitro drug release from the NLC of CSPE was done in PBS (pH 6.8 at 37 °C) by the use of the dialysis bag technique over 24 h. The in vitro release profiles of CSPE-NLC based cream and pure CSPE extract-based creams are shown in Fig. 4. Data of the release profiles prove that the developed CSPE-NLC was quite capable to release Hesperidin in a controlled mode since the cumulative release percentage over 24 h reached 90% Fig. 5.

### 3.6. Results of the experimental study

#### 3.6.1. Effect of the CSPE formulations on tissue level of collagen type I in the different experimental groups

UV radiation led to a severe loss of collagen demonstrated by the significant reduction in collagen levels in the UV injured group compared to the normal control group. Whereas, CSPE was able to significantly increase the levels of collagen in the skin tissue in the CSPE-NLC formulation group and the pure CSPE- cream group compared to the UV injured group (Fig. 6A).

#### 3.6.2. Effect of the CSPE formulations on tissue level of elastin in the different experimental groups

UV radiation significantly increased the elastin content in the skin tissue in the UV injured group compared to the normal control group. CSPE- NLC was able to significantly reduce elastin levels compared to the UV injured group and there was no significant difference between the standard, CSPE- NLC, and pure CSPE groups (Fig. 6B).

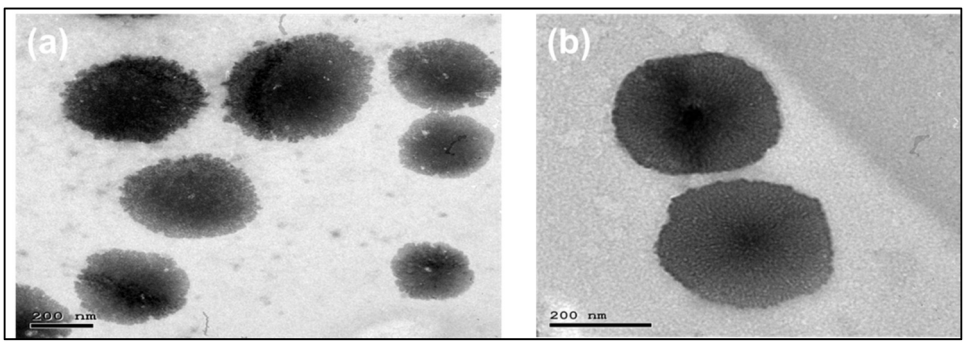


**Fig. 2.** TEM images of a) CSPE-SLN and b) CSPE-NLC.

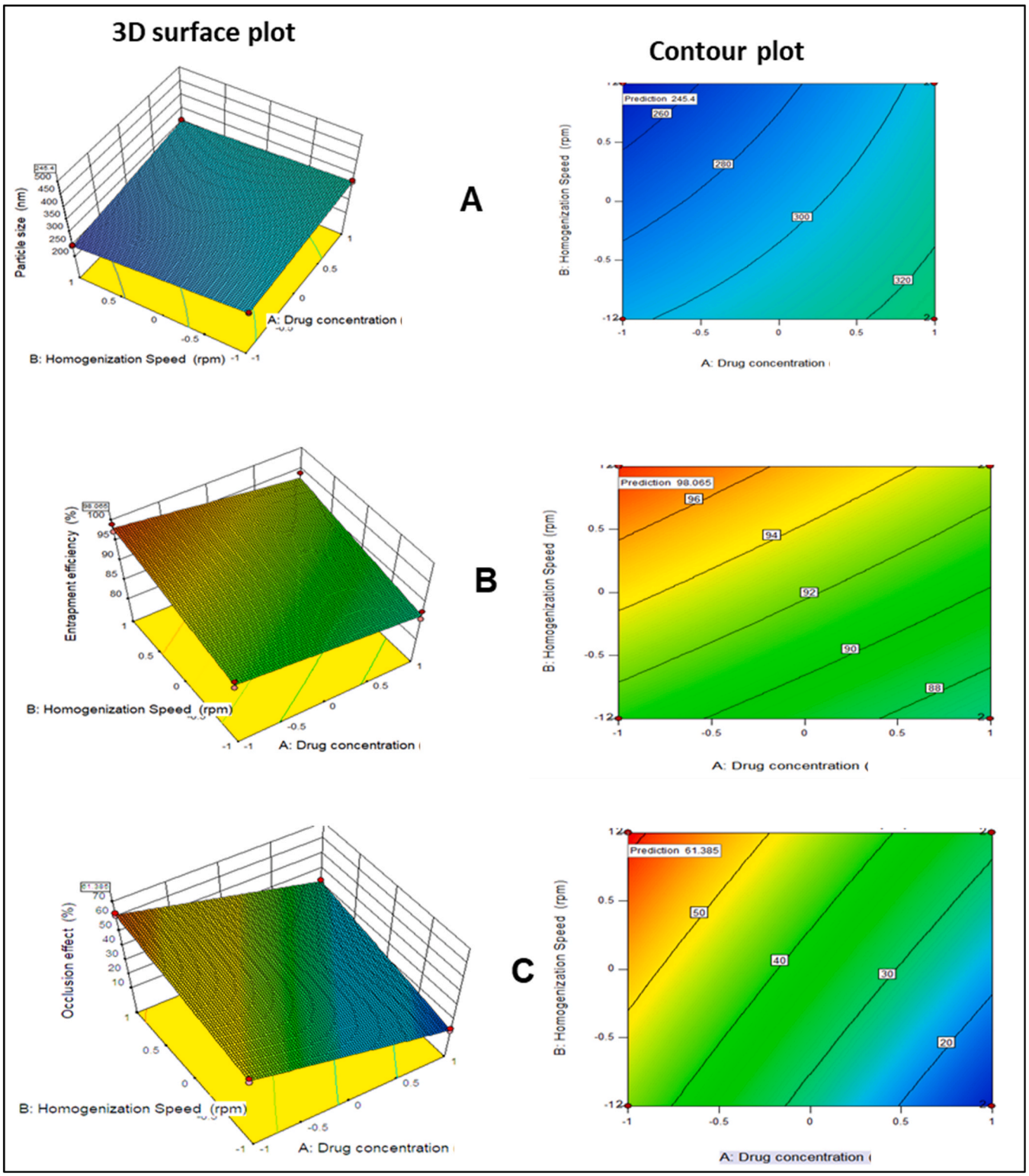


**Fig. 3.** 3D surface plots and contour plots for the effect of the studied variables on: **A-**particle size (Y1), **B-**entrapment efficiency (Y2), **C-** occlusion effect (Y3) of the prepared CSPE-NLC.

*3.6.3. Effect of the CSPE formulations on tissue level of COX-2 in the different experimental groups*

UV radiation triggered a significant elevation in the levels of COX-2 activity compared to the normal control group. The CS NLS formula resulted in a significant decline in the levels of COX-2 activity compared to the UV injured group (Fig. 6C).

*3.6.4. Effect of the CSPE formulations on tissue level of PGE-2 in the different experimental groups*

UV radiation caused significant inflammation demonstrated by the elevated levels of PGE-2 in comparison to the normal control group. The CSPE-NLC produced a significant reduction in the levels of the inflammatory mediator PGE-2 compared to the UV injured group (Fig. 6D).

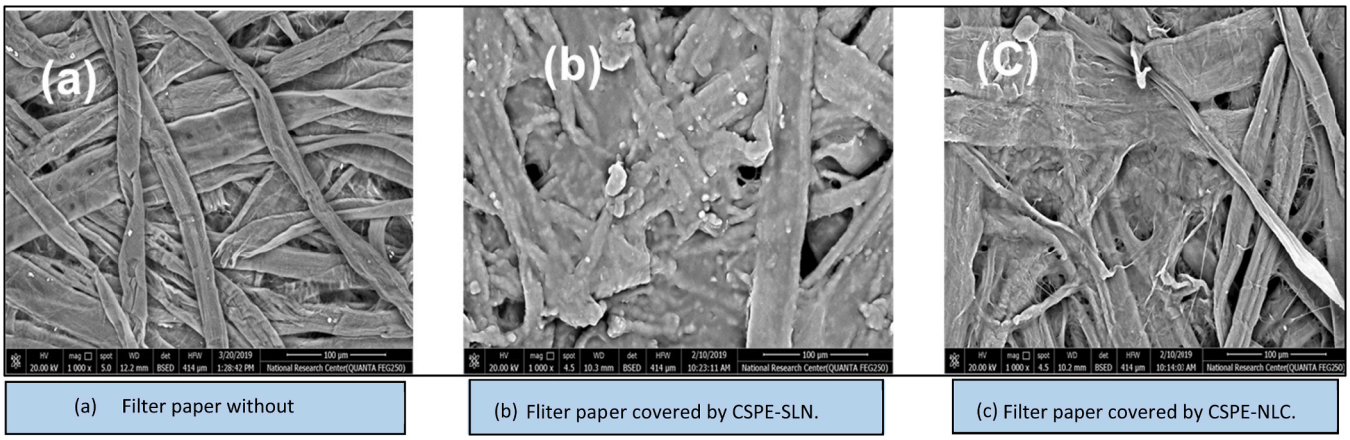


**Fig. 4.** SEM images showing occlusion effect of the LNP on filter paper.

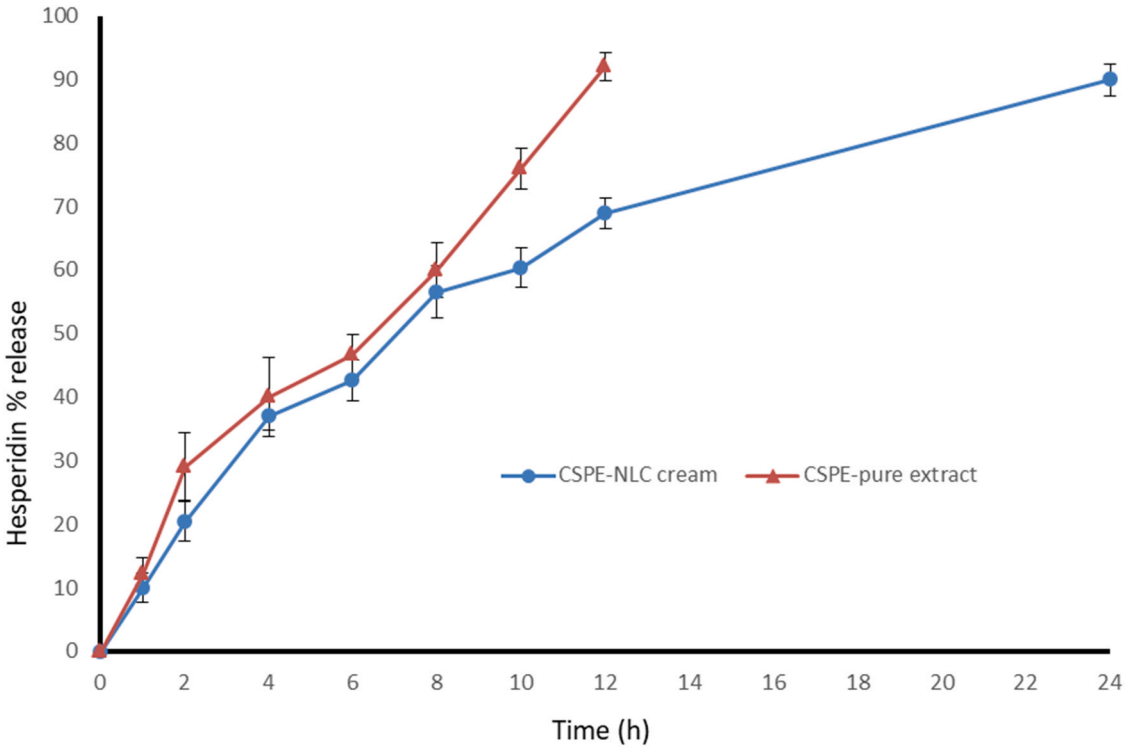


**Fig. 5.** *In- vitro* release profiles of Hesperidin from the prepared CSPE-NLC based cream and pure CSPE extract based creams in PBS of pH 6.8.

*3.6.5. Effect of the CSPE formulations on tissue level of JNK in the different experimental groups*

UV radiation caused a significant increase in the levels of JNK compared to the normal control group. The CSPE was able to significantly reduce the levels of JNK in the CSPE-NLC formulation group and the pure CSPE extract cream group compared to the UV injured group (Fig. 6E).

*3.6.6. Effect of the CSPE formulations on tissue level of SOD in the different experimental groups*

UV radiation was able to significantly reduce the levels of SOD compared to the normal control group. The CSPE- NLC formula was able to significantly improve the levels of the antioxidant machinery SOD compared to the UV injured group and produced results more significant than those of the standard marketed formula thereby reducing oxidative tissue damage induced by photo-aging (Fig. 6F).

*3.6.7. Effect of the CSPE formulations on tissue level of MDA in the different experimental groups*

UV radiation caused a significant elevation in the levels of MDA compared to the normal control group. The CSPE-NLC caused a significant reduction in the levels of MDA compared to the UV injured group. Also, it showed a significant decrease in the MDA levels compared to the standard marketed formulation and well as the pure CSPE extract formula (Fig. 6G).

*3.6.8. Effect of CSPE formulations on the expression level of MMP 1 in the different experimental groups*

The mRNA expression of MMP1 was found to be significantly increased in UV injured group compared to the control group at $P < 0.05$, The CS NLC showed a significant reduction in the expression levels of MMP1 compared to the UV injured group at $P < 0.05$ (Fig. 6H).

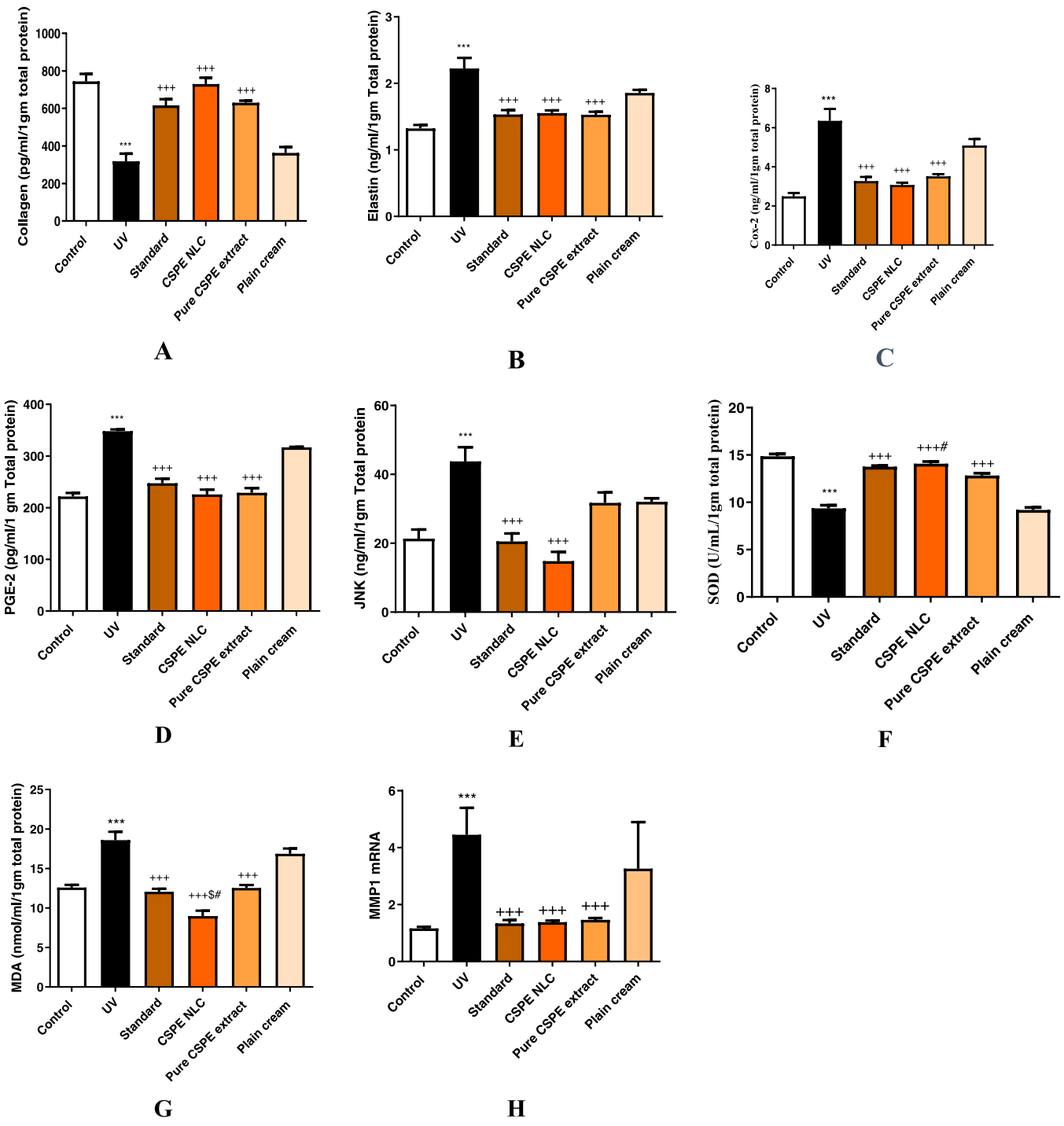


**Fig. 6.** Effect of standard cream, CS NLC formula, pure CS extract cream and plain cream treatment on levels of A-Collagen, B-Elastin, C- **COX-2, D-** PGE-2, E-JNK, F-SOD,G-MDA and H-MMP1 in skin homogenates of photoaged mice. Each result represents the mean value for 8 mice ± SE of the mean. Statistical analysis was carried out by one-way ANOVA followed by Tukey-Kramer multiple comparison test. ****statistically significant from the normal control group at* $p \leq 0.001$ *+++ statistically significant from the UV injured group at* $p \leq 0.001$.

### *3.6.9. Effect of CSPE formulations on the external appearance of the dorsal skin in the different experimental groups*

Fig. 7 shows the appearance of the dorsal skin of the mice, where Fig. 7A is the appearance of the normal healthy skin, Fig. 7B is the appearance of the skin after induction of photoaging and the appearance of wrinkles and Fig. 7C shows the improvement in the skin appearance after treatment with the CS NLC formula.

## 4. Discussion

There was always a significant link between skin aging and wrinkles and oxidative stress and solar radiations as well as several intrinsic and extrinsic factors.

Usually, there is a continuous process of formation and degradation of collagen and elastin fibers in the connective tissue done by normal skin to keep the dermal structure, however, oxidative stress decreases these fibers through Matrix metalloproteinase (MMP) or serine

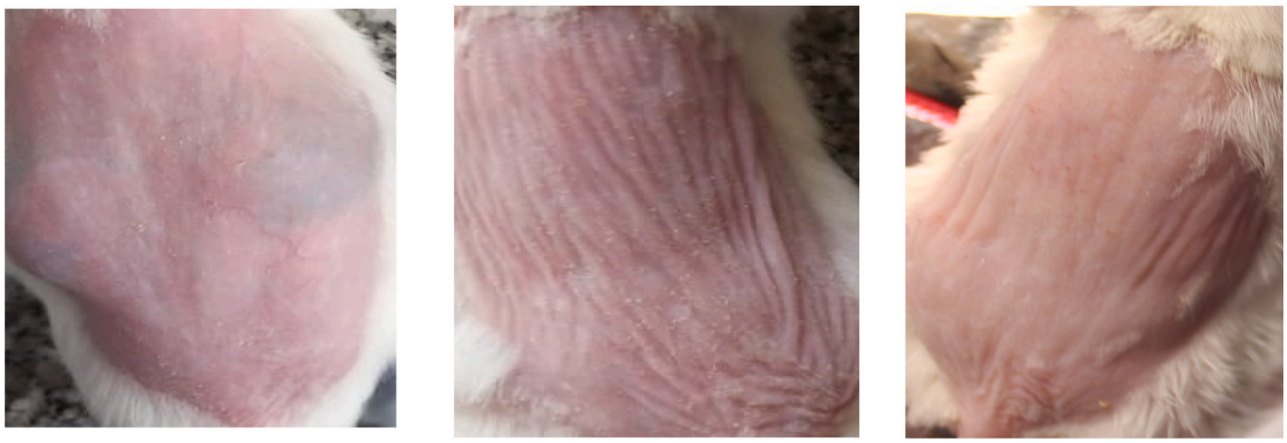


**Fig. 7.** Photographs for the dorsal side skin of mice: A-normal skin, B-Skin after wrinkle induction and C-skin after treatment.

proteinase pathways. MMPs are a family of endopeptidases responsible for the degradation of several extracellular matrix (ECM) components. This destruction has a detrimental effect on the skin and accelerates skin aging. Matrix metalloproteinase-1 (MMP-1) is classified as a collagenase [32], hence it is mainly responsible for the degradation and breakdown of collagen in the ECM. Ultraviolet (UV) radiation is among the stimuli that promote the expression of MMPs in general and MMP-1 specifically in dermal fibroblasts leading to photoaging [33], which makes MMP-1 inhibitors potential anti-aging compounds [34]. Elastase enzyme has been associated directly with collagen and elastin degradation and also indirectly through the activation of MMP-1 and MMP-2. [35] Therefore, natural products with well-established antioxidant activities could exhibit anti-elastase and anti-collagenase activity and consequently play a very essential role in anti-aging skin formulations. In our research, the ethanolic extracts of the *C. sinensis* L. fruit peels were characterized via HPLC-QToF-MS-MS and it was found that the majority of the metabolites are polyphenolic compounds which attribute to the CSPE antioxidant activity. CSPE showed promising antioxidant activity with $ED_{50}$ of (30.12 ± 3.59 μg/mL) and inhibited the elastase and collagenase enzymes with $IC_{50}$ values of (299.04 μg/mL and 188.61 μg/mL) respectively. *C. reticulate* fruit peels extract showed similar antioxidant, anti-elastase, and anti-collagenase results as reported in an in vitro study by [36]. Also, in agreement with our results, [37] reported that a mixture of citrus juices and its active ingredients exhibited potent antioxidant and anti-aging effects in hairless mice and human dermal fibroblasts.

A recent study by [38] compared the peel and seeds extracts of Lime (*Citrus amblycarpa*) for their inhibitory activity on elastase enzyme and found that the peel extract possessed a lower $IC_{50}$ value of 36.94 μg / mL compared to 62.39 μg / mL for the seed extract. However, when evaluating the activity of *Citrus unshiu* fruit bulbs, it showed higher collagenase and elastase inhibition than the peels [39].

No previous studies could be traced to evaluate the collagenase inhibitory activity of the individual compounds identified in CSPE via HPLC-QToF-MS except for hyperoside that showed an inhibitory activity with IC50 = 1.7 ± 0.04 [40]. However, [41] stated that flavonols were proven to be more potent inhibitors than the flavone and isoflavones, implying that the C-3-hydroxyl group in the compounds is essential for the activity and flavanones did not show significant inhibition at concentrations up to 100 pM. In agreement with these findings [42], added that at a specific concentration of (0.2 mM) the collagenase activity was inhibited by quercetin (21.1 ± 1.2%), kaempferol (12.5 ± 0.7%), apigenin (14.5 ± 0.5%), and luteolin (11.1 ± 0.8%). Moreover, the weak inhibitory activity of isoflavones was recently evidenced by [43] reporting that genistein showed a collagenase inhibitory activity with (IC50 = 98.74 ± 4.25 ug/mL). Concerning the polyphenolic compounds, resveratrol was evaluated as an anti-collagenase at a concentration of 5 μM was found to inhibit it by 22.47 ± 0.63 [44].

No doubt that particle size is of the most important features of the nanoparticles which has a dual effect on both the release pattern of the drug and its absorption. Average particle size, polydispersity, and zeta potential are shown in Table 2. The results revealed that the size distribution of prepared CSPE-SLN and CSPE-NLC is in the nano-size range. Sizes ranged from 237.8 ± 9.2 nm to 476.9 ± 17. PDI indicates the width of the particle size distribution. Theoretically, monodisperse distributions are represented as PDI = 0, however, PDI < 0.2 is considered as narrow size distribution [45]. PDI > 0.2 for the lipid nanoparticles prepared could be due to the preparation method used, giving a wide size distribution [46]. Furthermore, all formulae showed negative zeta potential based on the fact that lipid nanoparticles have a negative charge on their surface as a result of the presence of terminal carboxylic groups in the lipids [47]. Values of Zeta potential of most of the formulae are ranged around the desired ± 30 mV, which may reflect physical stability issues during storage [48]. Additionally, the Transmission Electron Microscopy (TEM) morphological examination for the prepared LNPs confirmed this finding as shown in Fig. 1. The morphological examination revealed that particles were spherical and uniform with the absence of any aggregates.

The model indicates that when using higher drug concentration with a fixed amount of surfactant these lead to building higher particle size. This may be as a result of the fact that the concentration of surfactant will have a limited effect of reducing the PS, as higher surfactant concentration stabilizes the lipid matrix successfully through the development of a steric barrier on their surface, thus avoiding aggregation and decrease the PS . In addition to that, the homogenization speed had also a remarkable effect which is attributed to the increased shear provided to break the globules and decrease the PS. On the other hand, the addition of liquid lipid (in NLC formulae) was found to cause a decrease in particle size compared to SLN. stated that the incorporation of 30% liquid lipid caused a marked decrease in particle size compared to corresponding SLN.

Based on the results showed in Table 2, the Hesperidin entrapment efficiency for all formulae was ranged from 80.45 to 97.23%. The model shows that increasing drug concentration leads to a decrease in the EE. Overall, high EE was the result of the high solubility of the drug in the melted lipid by aiding of surfactant [49]. Therefore, by increase in drug content that causes lowering the surfactant ratio with lowering of its availability to keep the drug sufficiently entrapped in the lipid leading to its discharge and lower EE. Concerning the homogenization speed factor ($X_2$) the EE increased with decreasing the speed as can be deduced from the negative coefficient of B. This could be explained by applying higher kinetic energy on formerly prepared lipid particles that may bring out

the entrapped drug into the aqueous medium, causing low entrapment efficiency [50]. On the other hand, $X_3$ (nanoparticle type) had a negative coefficient of C, which indicate that by using the NLC as carrier the EE of the system will increase. The high EE of NLC compared to SLN could be due to the addition of liquid lipid in NLC leading to a less ordered inner structure which allows more Hesperidin to be incorporated inside the NLC matrix [31].

As far as cosmetics topical administration is concerned, an interesting privilege of SLNs and NLCs is their occlusive effect, which has been related to their distinctive properties [51,52]. Lipid nanoparticles tend to undergo fusion which leads to the formation of a film on the skin [53]. This effect also occurred on the filter paper as confirmed by Scanning electron microscopy in Fig. 3. This film is thought to be responsible for the occlusive effect observed in the test since it acts like a barrier that avoids water vapor to escape through the filter paper. As reported in the literature, in vitro occlusion effects of the lipid nanoparticles are improved in correspondence to increase of the lipid concentration or decrease in the particle size [51,53]. This is due to the fact that the ability of lipid particles to form the protecting film on the skin is enhanced.

It is obvious from Eq. (3); the highest occlusion factor was obtained by decreasing the level of factor ($X_1$) and by increasing the level of ($X_2$) factor and by using NLC. Interestingly, this finding is in accordance with that previously demonstrated, the degree of occlusion of these films depends on the particle size [54]. As the particle size is decreased by lowering the level of drug concentration($X_1$) and by using NLC ($X_3$) as can be assumed from the negative coefficient of A and C. Contour plots and 3D surface plots were obtained by fixing the $X_3$ factor using CSPE-NLC and varying the $X_1$ and $X_2$ factors over the ranges used in the factorial study as showed in Fig. 2.

Subsequently and according to our $2^3$ full factorial experimental design, the selection of the optimized formula is based on the highest desirability factor calculated by design expert 7.0 software for achieving the desired criteria of particle size (200−300) and the maximum value of both EE, and occlusive effect. The software Design Expert 7.0.0 suggested optimum formula from variables values of 500 mg CSPE ($X_1$ = Drug concentration) and 15,000 rpm ($X_2$ = Homogenization Speed) and NLC ($X_3$ = nanoparticle type). Remarkably, F7 (CSPE-NLC) in this study fulfills the parameters needed for the suggested optimized formula. The observed values for the suggested formula are 245.4 nm (PS), 98.065% (EE), 61.385%( occlusion effect) with desirability reach 0.962. Finally, these results confirm the reliability of the optimization procedure followed in the present study to prepare formulations according to the $2^3$ full factorial design. Furthermore, the optimized prepared formula of CSPE-NLC dispersion was converted into a cream carrier system using stearic acid as a lipid base for subsequent pharmacological study for the anti-aging effect of *Citrus sinensis* Peel Extract(CSPE).

Generally speaking, drug release is a crucial step during the development stages of a new formulation and is considered as a routine quality control test for assuring final uniformity of finished product. The in vitro release profiles of CSPE-NLC based cream and pure CSPE extract-based creams are shown in Fig. 4. Data on the release profiles confirm that developed CSPE-NLC could release Hesperidin in a controlled mode as the cumulative release percentage over 24 h reached 90%. On the other hand, the pure CSPE extract-based cream reaches a 90% release of the active moiety within 12 h only. That slow release of the hesperidin from CSPE-NLC based cream is evidence of homogeneous entrapment of the drug throughout the systems. In addition to that, the process of incorporation of nanoparticulate dispersion into cream caused a further decrease in the drug release. Most probably this result was a result of the release retarding effect of the lipid phase of the cream [55]. Additionally, it is obvious that both release profiles, are biphasic release behavior, exhibiting a relatively rapid release within the first hours (35%) followed by a more retarded release pattern evidenced.

To shed the light on the mechanism of action of CSPE, we assessed the levels of COX-2, PGE-2, Elastin, Collagen type 1, C-JNK-1, MDA, SOD, and the genetic expression of MMP-1 in skin tissue. Levels of C-JNK were increased significantly in the UV-injured group compared to the control group. Also, the mRNA expression of MMP1 was significantly increased, which in turn lead to a significant decrease in collagen levels in the UV-injured group compared to the control group, while treatment with CSPE-NLC significantly decreased MMP1 and elevated collagen levels compared to the UV-injured group. UV irradiation stimulates the production and generation of excess reactive oxygen species (ROS) which in turn induces the synthesis and expression of MMP-1 by dermal fibroblasts. ROS also activates mitogen-activated protein kinases (MAPK) leading to the upregulation of C-JNK and activation of the transcription factor AP-1 which upregulates the expression of MMP-1 thereby causing the degradation of collagen in skin tissue [56]. Our results are in agreement with a study carried out by [57] who found that the pretreatment of the fibroblast with *Neonauclea reticulata* water extract resulted in a significantly reduced level of MMP_1 expression and increased level of the collagen. Another study was performed by [58] in which the ethanol extract of *Kaempferia parviflora* Wall. ex. Baker (black ginger) on UVB-induced photoaging in vivo leads to increased collagen type 1 via the suppression of c-JNK and c-Fos activity. The levels of Cox-2 and PGE-2 were significantly elevated in UV-injured group compared to control group, meanwhile treatment with CS-NLC significantly reduced both levels compared to UV-injured group.

COX-2 is the rate-limiting enzyme in the arachidonic acid pathway. UV radiation stimulates intracellular ROS and enhances COX-2 expression by p38 MAPK activation which in turn elevates PGE2 production. Our results are in agreement with Park et al., 2014, in which the ethanol extract of *Kaempferia parviflora* on UVB-induced photoaging in vivo leads to decreased expression of inflammatory mediators (nuclear Factor-B), interleukin-1 B, and Cox-2 activity. Another study [59], showed that the polymethoxy flavonoids in citrus peel extract significantly suppressed Cox-2 expression and PGE-2 production in HaCaT cell line. On the other hand, the level of elastin was significantly increased in the UV-injured group compared to the control group, meanwhile, the treatment with CS-NLC significantly reduced its level compared to the UV-injured group.

UV exposure leads to enhancement of elastin biosynthesis, which might be attributed to the activation of elastin promotor, where the accumulation of poorly organized elastin named solar-elastosis is the major histopathological alteration in photo-aging skin. In agreement to our study, in which the elastin production was increased after UV exposure which results in the accumulation of abnormal elastic materials in the skin in mice [60].

## 5. Conclusion

The processing of food waste enforces a burden on factories and causes enormous environmental problems. Citrus fruits- orange in particular- are one of the most vital merchandises with regards to global agricultural production. Citrus wastes are about 45–50% of the weight of citrus. Since Navel orange (*Citrus sinensis*) is the major citrus crop in Egypt. Herein, we implement the beneficial reuse of *Citrus sinesis* L. peel standardized extract in the management of photo-aging applying nanoparticle technology to enhance its efficacy. Our results revealed that the CSPE exhibited potent anti-aging activity via downregulation of mRNA expression of MMP1, anti-inflammatory, and anti-oxidant effects. This work highlights the reuse of waste as an alternative solution to the problems accompanying environmental pollution, by extracting bioactive eco-friendly extracts in stable nano formula with high added value. Further clinical trials are recommended to rationalize their use in the market.

## Conflict of interest statement

The authors have no conflict to declare.

## References


[1] J. Varani, R.L. Warner, M. Gharaee-Kermani, S.H. Phan, S. Kang, J. Chung, Z. Wang, S.C. Datta, G.J. Fisher, J.J. Voorhees, Vitamin a antagonizes decreased cell growth and elevated collagen-degrading matrix metalloproteinases and stimulates collagen accumulation in naturally aged human skin1, J. Invest. Dermatol. 114 (3) (2000) 480–486.

[2] S. Cho, M.H. Shin, Y.K. Kim, J.-E. Seo, Y.M. Lee, C.-H. Park, J.H. Chung, Effects of infrared radiation and heat on human skin aging in vivo, J. Invest. Dermatol. Symp. Proc. 14 (2009) 15–19.

[3] S. Saraf, C. Kaur, Phytoconstituents as photoprotective novel cosmetic formulations, Pharmacogn. Rev. 4 (7) (2010) 1.

[4] R. Hooda, Antiwrinkle herbal drugs@ An update, J. Pharmacogn. Phytochem. 4 (2015) 277–281.

[5] S.S. Liew, W.Y. Ho, S.K. Yeap, S.A.B. Sharifudin, Phytochemical composition and in vitro antioxidant activities of Citrus sinensis peel extracts, PeerJ 6 (2018), e5331 e5331-e5331.

[6] W. Abobatta, Improving navel orange (Citrus sinensis L) productivity in Delta Region, Egypt, Adv. Agr. Environ. Sci. 2 (1) (2018) 8–10.

[7] W.F. Abobatta, Overview of Role of Magnetizing Treated Water in Agricultural Sector Development, 2019.

[8] A.P. Nikam, M.P. Ratnaparkhiand, S.P. Chaudhari, Nanoparticles – an overview, Int. J. Res. Dev. Pharm. L. Sci. 3 (2014) 1121–1127.

[9] A. Pezeshki, B. Ghanbarzadeh, M. Mohammadi, I. Fathollahi, H. Hamishehkar, Encapsulation of vitamin a palmitate in nanostructured lipid carrier (NLC)-effect of surfactant concentration on the formulation properties, Adv. Pharm. Bull. 4 Suppl 2 (2014) 563–568.

[10] S.H. Ansari, F. Islam, M. Sameem, Influence of nanotechnology on herbal drugs: a review, J. Adv. Pharm. Technol. Res. 3 (3) (2012) 142–146.

[11] T. Mishra, A.P. Das, A. Sen, Phytochemical screening and ln-vitro antioxidant profiling of solvent fractions of canna edulis ker gawler, Free Radic. Antioxid. 2 (1) (2012) 13–20.

[12] C. Lucas-Abellán, M. Mercader Ros, M. Zafrilla, M. Fortea, J. Gabaldon, E. Núñez-Delicado, ORAC-fluorescein assay to determine the oxygen radical absorbance capacity of resveratrol complexed in cyclodextrins, J. Agric. Food Chem. 56 (2008) 2254–2259.

[13] T.S. Thring, P. Hili, D.P. Naughton, Anti-collagenase, anti-elastase and anti-oxidant activities of extracts from 21 plants, BMC Complement. Altern. Med. 9 (1) (2009) 27.

[14] V. Teeranachaideekul, P. Boonme, E.B. Souto, R.H. Muller, V.B. Junyaprasert, Influence of oil content on physicochemical properties and skin distribution of Nile red-loaded NLC, J. Control. Release 128 (2) (2008) 134–141.

[15] G.E. Yassin, M.H. Sayed, Statistical optimization of fluconazole-loaded vesicular systems for the treatment of skin fungal infections, Int J. Pharm. Sci. Sci. Res. (2018) 10–23.

[16] S. Dzulhi, E. Anwar, T. Nurhayati, Formulation, Characterization and In Vitro Skin Penetration of Green tea ( Camellia sinensis L.) Leaves Extract-Loaded Solid Lipid Nanoparticles, J. Appl. Pharm. Sci. 8 (8) (2018) 57–62.

[17] S. Dzulhi, E. Anwar, T. Nurhayati, Formulation, characterization and in vitro skin penetration of green tea (Camellia sinensis L.) leaves extract-loaded solid lipid nanoparticles, J. Appl. Pharm. Sci. 8 (08) (2018) 057–062.

[18] Y. Dong, W.K. Ng, S. Shen, S. Kim, R.B. Tan, Preparation and characterization of spironolactone nanoparticles by antisolvent precipitation, Int. J. Pharm. 375 (2009) 84–88.

[19] A.S. Dhase, S.S. Khadbadi, S.S. Saboo, Formulation and evaluation of vanishing herbal cream of crude drugs, Am. J. Ethnomed. 1 (2014) 313–318.

[20] V.B. Pokharkar, P.B. Shekhawat, V.V. Dhapte, L.P. Mandpe, Development and optimization of eugenol loaded nanostructured lipid carriers for periodontal delivery, Int. J. Pharm. Pharm. Sci. 3 (4) (2011) 138–143.

[21] K.M. Kamel, I.A. Khalil, M.E. Rateb, H. Elgendy, S. Elhawary, Chitosan-coated cinnamon/oregano-loaded solid lipid nanoparticles to augment 5-fluorouracil cytotoxicity for colorectal cancer: extract standardization, nanoparticle optimization, and cytotoxicity evaluation, J. Agric. Food Chem. 65 (36) (2017) 7966–7981.

[22] S. Sharma, I.P. Kaur, Development and evaluation of sesamol as an antiaging agent, Int. J. Dermatol. 45 (3) (2006) 200–208.

[23] K.C. Chang, Q. Shen, I.G. Oh, S.A. Jelinsky, S.F. Jenkins, W. Wang, Y. Wang, M. LaCava, M.R. Yudt, C.C. Thompson, L.P. Freedman, J.H. Chung, S. Nagpal, Liver X receptor is a therapeutic target for photoaging and chronological skin aging, Mol. Endocrinol. 22 (11) (2008) 2407–2419.

[24] I.S. Hwang, J.E. Kim, S.I. Choi, H.R. Lee, Y.J. Lee, M.J. Jang, H.J. Son, H.S. Lee, C. H. Oh, B.H. Kim, S.H. Lee, D.Y. Hwang, UV radiation-induced skin aging in hairless mice is effectively prevented by oral intake of sea buckthorn (Hippophae rhamnoides L.) fruit blend for 6 weeks through MMP suppression and increase of SOD activity, Int. J. Mol. Med. 30 (2) (2012) 392–400.

[25] T.K. Bhattacharyya, M. Pathria, C. Mathison, M. Vargas, J.R. Thomas, Cosmeceutical effect on skin surface profiles and epidermis in UV-B-irradiated mice, JAMA Fac. Plast. Surg. 16 (4) (2014) 253–260.

[26] H. ICH, Validation of analytical procedures: text and methodology, Q2 (R1). Current Step 4 Version, Parent Guidelines on Methodology Dated November 6 1996. Incorporated in November 2005, International Conference on Harmonisation of Technical Requirements for Registration of Pharmaceuticals for Human Use, Geneva, Switzerland, 2005.

[27] A.M. El-Shafae, M.M. El-Domiaty, Improved LC methods for the determination of diosmin and/or hesperidin in plant extracts and pharmaceutical formulations, J. Pharm. Biomed. Anal. 26 (4) (2001) 539–545.

[28] L.H. Keith, L.U. Gron, J.L. Young, Green analytical methodologies, Chem. Rev. 107 (6) (2007) 2695–2708.

[29] H.M. MoHaMed, N.T. Lamie, Analytical eco-scale for assessing the greenness of a developed RP-HPLC method used for simultaneous analysis of combined antihypertensive medications, J. AOAC Int. 99 (5) (2016) 1260–1265.

[30] J. Płotka-Wasylka, A new tool for the evaluation of the analytical procedure: green analytical procedure index, Talanta 181 (2018) 204–209.

[31] W. Mehnert, K. Mäder, Solid lipid nanoparticles: production, characterization and applications, Adv. Drug Deliv. Rev. 64 (2012) 83–101.

[32] T. Ishchuk, D. Glavachek, O. Savchuk, P. Yakovlev, T. Falaleeva, T. Beregova, L. Ostapchenko, Plasma levels of MMPs and TIMP-1 in urinary bladder cancer patients, Biomed. Res. Ther. 5 (1) (2018) 1931–1940.

[33] S. Shin, S.H. Cho, D. Park, E. Jung, Anti-skin aging properties of protocatechuic acid in vitro and in vivo, J. Cosmet. Dermatol. 19 (4) (2020) 977–984.

[34] E.J. Shin, S. Jo, H.K. Choi, S. Choi, S. Byun, T.G. Lim, Caffeic acid phenethyl ester inhibits UV-induced MMP-1 expression by targeting histone acetyltransferases in human skin, Int. J. Mol. Sci . 20 (12) (2019).

[35] S.Y. Itoh, M. Shigeyama, K. Sakaguchi, I, The anti-aging potential of extracts from chaenomeles sinensis, Cosmetics 6 (1) (2019) 21.

[36] V. Apraj, N. Pandita, Evaluation of skin anti-aging potential of Citrus reticulata blanco peel, Pharmacogn. Res. 8 (3) (2016) 160–168.

[37] D.-B. Kim, G.-H. Shin, J.-M. Kim, Y.-H. Kim, J.-H. Lee, J.S. Lee, H.-J. Song, S. Y. Choe, I.-J. Park, J.-H. Cho, O.-H. Lee, Antioxidant and anti-ageing activities of citrus-based juice mixture, Food Chem. 194 (2016) 920–927.

[38] S. Stevenie, E. Girsang, A.N. Nasution, I.N.E. Lister, Comparison activities of peel and extract of lime (Citrus amblycarpa) as antioxidant and antielastase, Am. Sci. Res. J. Eng. Technol. Sci. 57 (2019) 77–84.

[39] K.M.-S. Eun C-H, I.-J. Kim, Elastase/collagenase inhibition compositions of citrus unshiu and its association with phenolic content and anti-oxidant activity, Appl. Sci. 10 (14) (2020), 4838.

[40] T. Kawaguchi, K. Nagata, Collagenase inhibition by water-pepper (Polygonum hydropiper L.) sprout extract, J. HerbMed Pharmacol. 8 (2019) 114–119.

[41] B. Sin, H. Kim, Inhibition of collagenase by naturally-occurring flavonoids, Arch. pharm. Res. 28 (2005) 1152–1155.

[42] G.S. Sim, B.C. Lee, H.S. Cho, J.W. Lee, J.H. Kim, D.H. Lee, J.H. Kim, H.B. Pyo, D. C. Moon, K.W. Oh, Y.P. Yun, J.T. Hong, Structure activity relationship of antioxidative property of flavonoids and inhibitory effect on matrix metalloproteinase activity in UVA-irradiated human dermal fibroblast, Arch. Pharm. Res. 30 (3) (2007) 290–298.

[43] W. Geeta, W. Widodo, C. Widowati, I. Ginting, A. Lister, E. Armansyah, Comparison of antioxidant and anti-collagenase activity of genistein and epicatechin, Pharm. Sci. Res. 6 (2019).

[44] S. Giardina, A. Michelotti, G. Zavattini, S. Finzi, C. Ghisalberti, F. Marzatico, Efficacy study in vitro: assessment of the properties of resveratrol and resveratrol + N-acetyl-cysteine on proliferation and inhibition of collagen activity, Minerva Ginecol. 62 (2010) 195–201.

[45] S. Das, W.K. Ng, R.B. Tan, Are nanostructured lipid carriers (NLCs) better than solid lipid nanoparticles (SLNs): development, characterizations and comparative evaluations of clotrimazole-loaded SLNs and NLCs? Eur. J. Pharm. Sci. 47 (1) (2012) 139–151.

[46] R. López-García, A. Ganem-Rondero, Solid lipid nanoparticles (SLN) and nanostructured lipid carriers (NLC): occlusive effect and penetration enhancement ability, J. Cosmet. Dermatol. Sci. Appl. 05 (02) (2015) 62–72.

[47] C. Schwarz, Solid lipid nanoparticles (SLN) for controlled drug delivery II. Drug incorporation and physicochemical characterization, J. Microencapsul. 16 (2) (1999) 205–213.

[48] E. Garzón, P. Sánchez-Soto, E. Romero, Physical and geotechnical properties of clay phyllites, Appl. Clay Sci. 48 (3) (2010) 307–318.

[49] K. Derakhshandeh, M. Erfan, S. Dadashzadeh, Encapsulation of 9-nitrocampto-thecin, a novel anticancer drug, in biodegradable nanoparticles: factorial design, characterization and release kinetics, Eur. J. Pharm. Biopharm. 66 (1) (2007) 34–41.

[50] M. Shah, D. Fawcett, S. Sharma, S.K. Tripathy, G.E.J. Poinern, Green synthesis of metallic nanoparticles via biological entities, Materials 8 (11) (2015) 7278–7308.

[51] S. Wissing, R. Müller, The influence of the crystallinity of lipid nanoparticles on their occlusive properties, Int. J. Pharm. 242 (1–2) (2002) 377–379.

[52] C. Loo, M. Basri, R. Ismail, H. Lau, B. Tejo, M. Kanthimathi, H. Hassan, Y. Choo, Research highlights: highlights from the last year in nanomedicine, Nanomedicine 8 (2013) 13–15.

[53] S. Wissing, A. Lippacher, R. Müller, Investigations on the occlusive properties of solid lipid nanoparticles (SLN), J. Cosmet. Sci. 52 (5) (2001) 313–324.

[54] S.A. Wissing, R.H. Müller, Cosmetic applications for solid lipid nanoparticles (SLN), Int. J. Pharm. 254 (1) (2003) 65–68.

[55] P.V. Pople, K.K. Singh, Development and evaluation of topical formulation containing solid lipid nanoparticles of vitamin A, AAPS Pharmscitech 7 (4) (2006) E63–E69.

[56] P. Pittayapruek, J. Meephansan, O. Prapapan, M. Komine, M. Ohtsuki, Role of matrix metalloproteinases in photoaging and photocarcinogenesis, Int. J. Mol. Sci. 17 (6) (2016) 868.

[57] H.-M. Chiang, H.-C. Chen, H.-H. Chiu, C.-W. Chen, S.-M. Wang, K.-C. Wen, Neonauclea reticulata (Havil.) Merr stimulates skin regeneration after UVB exposure via ROS scavenging and modulation of the MAPK/MMPs/collagen pathway, Evid. Based Complement. Altern. Med. 2013 (2013) 1–9.

[58] J.E. Park, H.B. Pyun, S.W. Woo, J.H. Jeong, J.K. Hwang, The protective effect of K aempferia parviflora extract on UVB-induced skin photoaging in hairless mice, Photodermatol. Photoimmunol. Photomed. 30 (5) (2014) 237–245.

[59] N. Yoshizaki, T. Fujii, H. Masaki, T. Okubo, K. Shimada, R. Hashizume, Orange peel extract, containing high levels of polymethoxyflavonoid, suppressed UVB-induced COX-2 expression and PGE 2 production in HaCaT cells through PPAR-γ activation, Exp. Dermatol. 23 (2014) 18–22.
[60] Y.Q. Chen, E.F. Bernstein, K. Tamai, K.J. Shepley, K.S. Resnik, H. Zhang, R. Tuan, A. Mauviel, J. Uitto, Enhanced elastin and fibrillin gene expression in chronically photodamaged skin, J. Invest. Dermatol. 103 (2) (1994) 182–186.
[61] G.H. Jang, H.W. Kim, M.K. Lee, S.Y. Jeong, A.R. Bak, D.J. Lee, J.B. Kim, Characterization and quantification of flavonoid glycosides in the Prunus genus by UPLC-DAD-QTOF/MS, Saudi J. Biol. Sci. 25 (8) (2018) 1622–1631.
[62] M.H. El Bishbishy, H.A. Gad, N.M. Aborehab, Chemometric discrimination of three Pistacia species via their metabolic profiling and their possible in vitro effects on memory functions, J. Pharm. Biomed. Anal. 177 (2020), 112840.
[63] B.R. Choi, K.K. Karna, Y.S. Shin, S.W. Lee, C.Y. Kim, H.K. Kim, J.K. Park, PO-01-018 comparative pharmacokinetic and bioavailability studies of monotropein, kaempferol 3-O-glucoside and quercetin 4′-O-glucoside after oral and intraveneous administration of MOTILIPERM in rats, J. Sex. Med. 16 (5) (2019) S53–S54.
[64] Y. Chen, H. Yu, H. Wu, Y. Pan, K. Wang, Y. Jin, C. Zhang, Characterization and quantification by LC-MS/MS of the chemical components of the heating products of the flavonoids extract in pollen typhae for transformation rule exploration, in: Molecules, 20, 2015, pp. 18352–18366.
[65] S.S. Elhawary, I.Y. Younis, M.H. El Bishbishy, A.R. Khattab, LC–MS/MS-based chemometric analysis of phytochemical diversity in 13 Ficus spp. (Moraceae): correlation to their in vitro antimicrobial and in silico quorum sensing inhibitory activities, Ind. Crops Prod. 126 (2018) 261–271.
[66] M.S.A. Aya Allah Osma, Atef A. El-Hela, Phytoconstituents and biological investigation of minuartia genculata graebn, Int. J. Green. Herb. Chem. 8 (4) (2019) 353–374.
[67] G. Negri, Dd Santi, R. Tabach, Chemical composition of hydroethanolic extracts from siparuna guianensis, medicinal plant used as anxiolytics in amazon region, Rev. Bras. De. Farmacogn. 22 (2012) 1024–1034.
[68] A. Brito, J. Ramirez, E.C. Areche, B. Sepúlveda, M. Simirgiotis, J, HPLC-UV-MS profiles of phenolic compounds and antioxidant activity of fruits from three citrus species consumed in Northern Chile, Molecules 19 (2014) 17400–17421.
[69] P. Geng, J. Sun, M. Zhang, X. Li, J.M. Harnly, P. Chen, Comprehensive characterization of C-glycosyl flavones in wheat (Triticum aestivum L.) germ using UPLC-PDA-ESI/HRMS(n) and mass defect filtering, J. Mass Spectrom.: JMS 51 (10) (2016) 914–930.
[70] R.O. Bakr, M.H. El, Bishbishy, profile of bioactive compounds of capparis spinosa var. aegyptiaca growing in Egypt, Rev. Bras. De. Farmacogn. 26 (4) (2016) 514–520.
[71] Y. Wang, Z. Xu, Y. Huang, X. Wen, Y. Wu, Y. Zhao, Y. Ni, Extraction, purification, and hydrolysis behavior of apigenin-7-o-glucoside from chrysanthemum morifolium tea, Molecules 23 (11) (2018), 2933.
[72] M.J. Simirgiotis, J. Benites, C. Areche, B. Sepúlveda, Antioxidant capacities and analysis of phenolic compounds in three endemic nolana species by HPLC-PDA-ESI-MS, Molecules 20 (6) (2015) 11490–11507.
[73] Z. Tian, M. Wan, Z. Wang, B. Wang, The preparation of genistein and LC-MS/MS on-line analysis, Drug Dev. Res. 61 (2004) 6–12.
[74] Y. He, Z. Li, W. Wang, S.R. Sooranna, Y. Shi, Y. Chen, C. Wu, J. Zeng, Q. Tang, H. Xie, Chemical profiles and simultaneous quantification of aurantii fructus by Use of HPLC-Q-TOF-MS combined with GC-MS and HPLC methods, Molecules 23 (9) (2018), 2189.
[75] R. Flamini, Recent applications of mass spectrometry in the study of grape and wine polyphenols, ISRN Spectrosc. 2013 (2013) 1–45.
[76] M. Stefova, A. Petkovska, S. Ugarkovic, J.P. Stanoeva, Strategy for optimized use of LC-MSn for determination of the polyphenolic profiles of applepeel, flesh and leaves, Arab. J. Chem. 12 (8) (2019) 5180–5186.
[77] F. Chen, X. Long, Z. Liu, H. Shao, L. Liu, Analysis of phenolic acids of Jerusalem artichoke (Helianthus tuberosus L.) responding to salt-stress by liquid chromatography/tandem mass spectrometry, Sci. World J. 2014 (2014) 1–8, 568043-568043.
[78] S.M. Ezzat, M.H. El Bishbishy, N.M. Aborehab, M.M. Salama, A. Hasheesh, A. A. Motaal, H. Rashad, F.M. Metwally, Upregulation of MC4R and PPAR-α expression mediates the anti-obesity activity of Moringa oleifera Lam. in high-fat diet-induced obesity in rats, J. Ethnopharmacol. 251 (2020), 112541.